Drivers of epithelial-mesenchymal transition in chronic obstructive pulmonary disease

By

Kaosia Nowrin

Submitted in fulfilment of the requirements for the Degree of Master of Pharmacy by Research, School of Medicine, University of Tasmania, August, 2015

Declaration

I hereby declare that this thesis contains no material which has been accepted for the award of any other degree or diploma in any university and, to the best of my knowledge, contains no material previously published or written by any other person unless due reference is made in the text of this thesis.

Kaosia Nowrin

University of Tasmania, Hobart

29th August, 2015

Acknowledgements

The author wishes to thank several people. I would like to express the deepest appreciation for my supervisor, Professor E Haydn Walters, who has shown the attitude and inspiration of a genius, he continually and persuasively conveyed a spirit of adventure in regard to medical research and knowledge. Without his supervision and constant help this thesis would not have been possible. I would also like to thank my other supervisors, Dr Rahul Patel and Dr Sukhwinder Singh Sohal for their guidance and support in completion of this project. I would like to show my appreciation to Mr Steve Weston, research laboratory manager, who taught me the necessary technical skills, and laboratory training required throughout the project, as well as his immense support to complete the thesis. Also, a big thanks to the participants who were kind enough to give us their samples; without their support, this study would not have been possible. In addition, thank you to the other members of the Respiratory Research Group, especially my friends Tricia Spafford, Mariya Ahmed and Pawan Grewal, who have given me tremendous support and encouragement throughout the year. Moreover, I would like to thank Dr Jo-Maree Courtney for her generous contribution to the scientific figures in this thesis. Last but not least, I would like to thank my parents, my brothers for whom I dedicate my respect and love of knowledge, and my father for his beautiful advice “Knowledge is power”, which has always been a catalyst for me to pursue knowledge.

Table of contents

Contents

List of figures

List of Tables

Chapter 1 – Introduction & Literature Review

1.1 Chronic obstructive pulmonary disease (COPD)

COPD is a chronic disease with a complex condition that involves a frequent mix of airway and lung parenchymal damage. The Global Initiative for Chronic Obstructive Lung Disease (GOLD 2014) has characterised it by *persistent airflow limitation that is usually progressive and associated with an enhanced chronic inflammatory response in the airways and the lung to noxious particles or gases*. The definition of COPD has been a bit confusing and controversial due to its difficult diagnostic procedures over the years until recently. It was stereotyped as being caused by inflammation and considered analogous to asthma (1). The current definition of COPD does not include the terms chronic bronchitis and emphysema. Chronic bronchitis is the inflammation involving cough and sputum production that is not always necessarily associated with airflow limitation. Emphysema, defined as destruction of the alveoli, a pathological feature of several structural abnormalities in COPD that can also be found in people with normal lung functions (GOLD 2014). However, it is reflected by a decline in gas-exchange rate of the alveoli of the lungs by a measurement of the O_2 (oxygen) or CO (carbon monoxide) transfer rate (diffusion capacity) and can cause worsening of airflow limitation in COPD.

1.1a Epidemiology and global impact of COPD

According to World Health Organization (WHO) estimates, 210 million people are affected by COPD, with one hundred million deaths in the 20th century. The WHO predicts that total deaths from COPD will rise by 30% over the next decade, as smoking becomes increasingly epidemic in third world countries, which justifies an intense study of the disease that is currently lacking (2). The amount of one in 10 Australians aged 40 or over is affected by COPD (Burden of Obstructive Lung Disease- BOLD) (3). Alarmingly, only half of these affected people are aware that they have the condition. Australia has one of the highest COPD death rates in the developed world, putting the country in the 3rd position of the 34 Organization for Economic Co-operation and Development (OECD) countries (4). COPD is also the 2nd leading cause of avoidable hospital admissions. In China, where more than 50% of the men smoke, COPD is the leading cause of death in rural areas and 4th in polluted urban areas (5). In 2005, more than 126,000 adults in the United States died from COPD (6), while 30% of all cancer deaths, including 90% of lung cancer deaths, can be attributed to tobacco use (Figure 1.1).

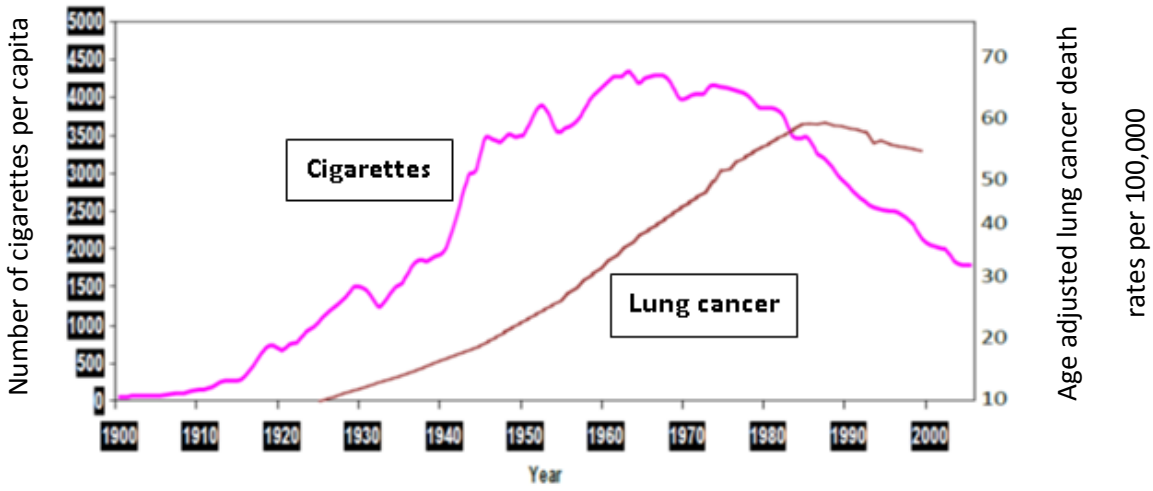

Figure 1.1 US cigarette use vs lung cancer deaths, 1900-2005 (Figure taken from Tobacco Outlook Report, Economic Research Service, US Department of Agriculture).

1.1b Clinical physiology

COPD is more than a "smoker's cough" or "chronic bronchitis". The diagnosis of COPD itself has to be confirmed by spirometry to demonstrate fixed airway obstruction. The presence of a post-bronchodilator ratio of forced expiratory volume in one second to forced vital capacity (FEV_1/FVC) <70% confirms the presence of airflow limitation that is not fully reversible and allows a diagnosis of COPD. The degree of FEV_1 decline defines the severity of the disease. The degree of Diffusing Capacity (Transfer Factor) decline caused by co-existing emphysema is not included in the physiological definition, though if present it will contribute to the airflow obstruction and also exacerbate symptoms (7).

Chronic cough, present intermittently or throughout the day, with or without chronic sputum production but without airflow obstruction, would formerly have been labelled chronic bronchitis, is now somewhat confusingly termed Stage 0 COPD (8). Stage 1 COPD with FEV_1 still at 80% or above is also usually largely asymptomatic. As the disease progresses into Stage II moderate COPD with FEV_1 between 50 and 80%, patients often experience shortness of breath, which may hamper their daily activities. As airflow limitation worsens and patients develop Stage III, or severe COPD, with FEV_1 less than 50%, the symptoms of cough and sputum production and especially shortness of breath typically worsen. In addition, COPD frequently exacerbates. Exacerbations are usually precipitated by an airway viral infection; cough and sputum first get worse and then breathlessness and then acute wheezing (9). Such acute exacerbations frequently land the patient in the hospital, and unfortunately this may be the first time a diagnosis of COPD is made (10). Indeed, much more attention needs to be given to primary care in case of finding the onset of the earlier stages of the disease, in order to intervene and stop this disastrous progression.

COPD classically involves three overlapping phenotypes related to the disease in the in-series structural components of the lung, i.e. in large (central) airways, small (peripheral) airways, and more variably the lung parenchyma (Figure 1.2). Large airways are defined as >4mm in internal diameter; they subdivide many times to become small airways, defined when the inner diameter becomes <2mm. After a total of about 23 divisions, the airways give rise to clusters of alveoli (small air sacs) that form the gas exchanging membrane in close association with blood in the pulmonary capillaries. These gas-exchanging tissue structures plus supporting matrix and connective tissue "skeletal" elements form the parenchyma of the lung. Thus, in gross summary, the current standard understanding of the pathologic changes in COPD lungs involve inflammation and thickening of large airways (bronchitis), fibrosis and obstruction of small airways (obstructive bronchiolitis) and destruction of the lung parenchyma (emphysema) (Figure 1.2). The early stages of the development of COPD can be diagnosed clinically by measuring FEV_1/FVC decline in early middle age of smokers and ex-smokers (11).

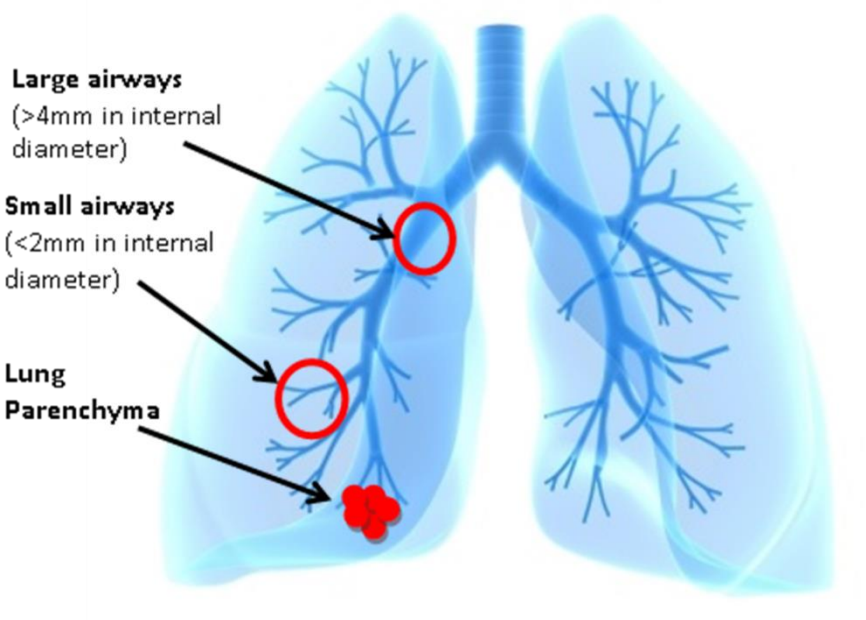

Figure 1.2 Respiratory tree (by Eraxion, iStock images)

1.1c Risk factors associated with COPD

COPD is largely caused by chronic exposure of the respiratory tract to harmful gases and particulates. Cigarette smoke is the major culprit in causing COPD in Western countries. The increased oxidant burden associated with depleted endogenous antioxidant defences occurs with each puff of a cigarette, containing more than 2,000 xenobiotic compounds and 10^{15} free radicals, causing damage to airways and lung epithelial cells (12). It has been demonstrated that cigarette smoking can induce pathological changes in the small airways even in smokers who have not yet developed symptoms of COPD (13). Smoking can activate many biological

processes at the cellular level which are potentially important in development of COPD (Figure 1.3) (14), and indeed chronic bronchitis.

In addition to cigarette smoking, repeated exposure to environmental and/or occupational pollutants, chronic (or latent) infection, or an interaction between these can also cause COPD. In third world countries where wood, peat and dung etc. are the main sources of indoor heating and cooking, exposure to such biomass smoke is also a major cause of COPD. Chronic active asthma also frequently leads to irreversible airflow obstruction, an effect that is synergistic with cigarette smoke damage (15).

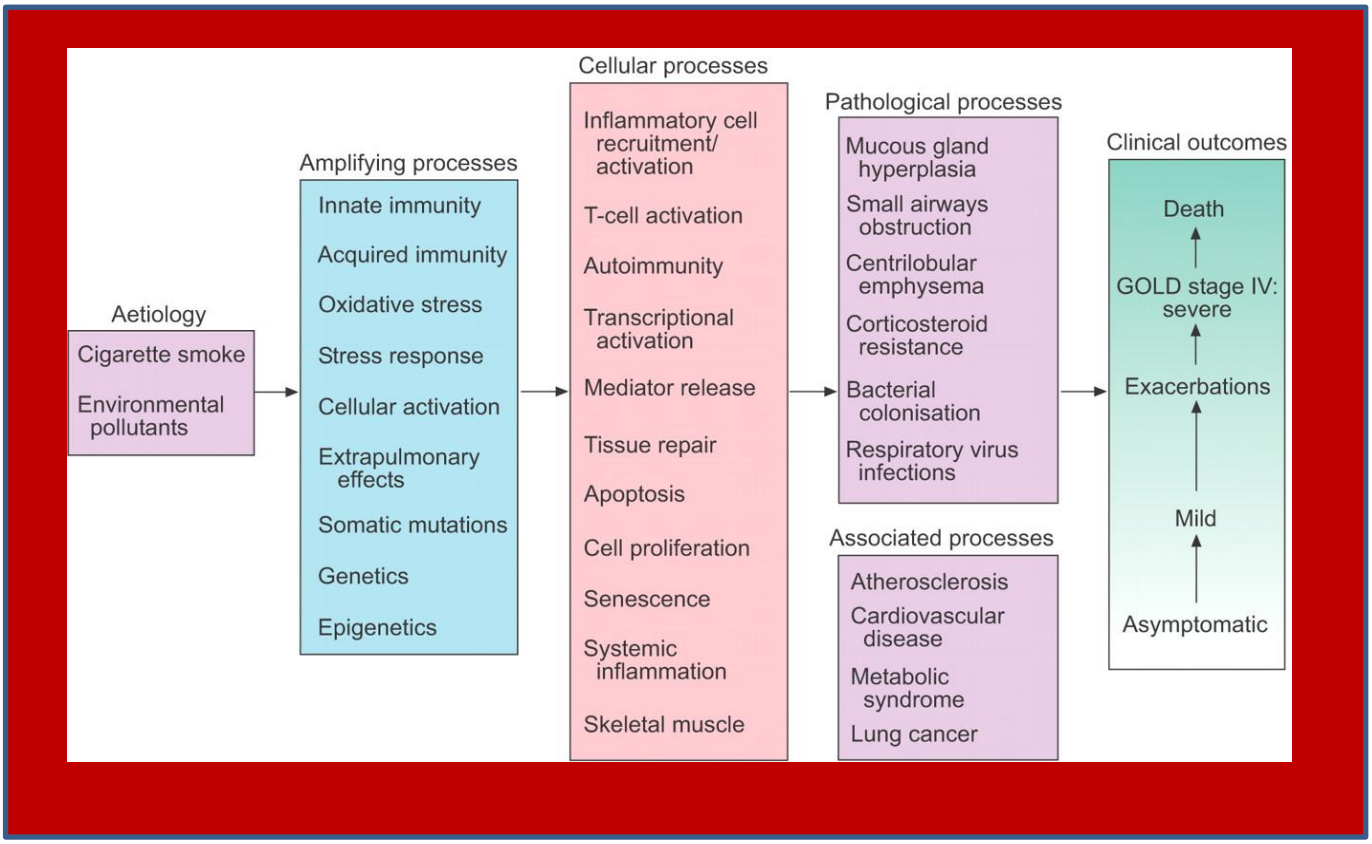

Figure 1.3 The link between smoking and pulmonary pathology.
Reproduced with permission (14).

1.2 Pathology of COPD

1.2a Background to pathology

Evolution of knowledge about COPD has occurred rapidly over the last few years. However, the history of COPD began in the nineteenth century with two landmark inventions- the stethoscope, by Laennec in 1819 and the spirometer, by Hutchinson in 1846. These offered new opportunities to discover the basic nature of COPD. Laennec was one of the first to recognise that a part of COPD is emphysema, where the lungs have lost their elasticity and empty poorly, with decreased elastic recoil pressure available to drive air out, accompanied by the abnormal destruction that begins in the small conducting airways, serving the alveoli of the lungs. "Perhaps both processes conspire to create the abnormality", he stated (16). Hutchinson's water spirometer allowed quantification of lung function, and he defined the vital capacity as "the number of cubic inches given by a full expiration following the deepest inspiration" (17). Spirometry was subsequently used to define the volume of air exhaled in the first second of maximum expiration and the ratio of this to the forced vital capacity (FVC), the forced expiratory ratio, has been used as the standard index of expiratory airflow obstruction.

Studies into the details of airway remodelling in the airways of COPD patients date back to the 1950s and 1960s. The pathologist Lynne Reid in the UK was one of the first to quantitate airway remodeling in COPD. Her careful assessments noted excessive mucus, which was associated with both an increase in the number of goblet cells and hypertrophy and hyperplasia of the mucus glands, with metaplasia in the epithelium in smokers and COPD subjects (18, 19). More recent pathological interest in smoker/COPD airways has focused on the concept that this is an inflammatory disease. In the sub-epithelial lamina propria (LP) area (100 microns deep to the epithelial reticular basement membrane) significant increases in CD3+ and CD8+ T lymphocytes have been demonstrated (20). Saetta *et al.* also found increased expression of macrophages and T-lymphocytes in both the epithelium and in the LP in chronic bronchitis subjects (21). The role of these cells is not well defined. Another type of inflammatory cell thought to be involved in airway remodelling in COPD is the mast cell, as these secretory cells can produce a number of bioactive factors including VEGF (vascular endothelial growth factor), bFGF (basic fibroblast growth factor), and many other pro-inflammatory, pro-fibrotic, anti-angiogenic factors (22). Study on mast cells in COPD airways showed greater mast cell density in all COPD groups compared to control subjects (non-smokers with normal lung function) and has been related to hyper-vascularity in smoking-related COPD subjects (23).

Although, there is an increase in mast cells, lymphocytes, and macrophages, there was a significant reduction in total cellularity in the LP of smokers and COPD patients (24). Neutrophils are prominent in mucous glands in COPD airways and neutrophil elastase secreted by these cells is potentially involved in airway remodelling (25). Neutrophils and macrophages are prominent in airway washings. However, neutrophils were decreased in the epithelium, reticular basement membrane (Rbm), and lamina propria (LP) in COPD-current smoker subjects (26). Neutrophils only go up generally in the airway wall with inhaled

corticosteroid treatment (27). In the last decade medical research on COPD has developed substantially. Although COPD is a pan-airway process, small airway fibrosis and obliteration are implicated as main contributors to the decline in lung function (28). This decline can be compounded by the later development of lung parenchymatous breakdown or emphysema in some patients. Airway changes in COPD have probably been over characterised by 'inflammation', and as analogous to asthma (1).

However, a recent description of epithelial to mesenchymal transition (EMT), the activation of airway epithelial cells to develop migratory and fibrotic characteristics, is contributing to understanding the complex picture of at least the airway components of COPD (29). EMT is a remarkable process where transitioning motile epithelial cells digest through the basement membrane (BM) and reticular basement membrane (RBM) to become we believe sub-epithelial fibroblasts, which could contribute to fibrosis by releasing extracellular matrix (ECM) proteins (Figure 1.4). These fibroblasts are also thought to stimulate the epithelium to further stimulate EMT, thus contributing to a vicious cycle of small airway narrowing and airflow obstruction. Most of this supposition comes from what we know about EMT in other epithelial situations, and more research is needed to work this out for COPD. EMT could also contribute to other important aspects of airway pathology; in particular, it has been recognised elsewhere as promoting formation of a pro-malignant microenvironment for epithelia (30-33), and so may be relevant to the development of lung cancer (34). A recent genetic study on smokers, COPD and lung cancer implicated a robust genomic link between COPD, lung cancer and Hedgehog signaling (35). Another very recent cohort study found that cancer in COPD patients was frequent, and under-diagnosis of COPD among patients with lung cancer was very high (68.3%) (36). In non-small-cell lung cancer, active EMT is associated with the formation of cancer stem cells (37), drug resistance, and epidermal growth factor receptor mutations (38). A large body of evidence supports EMT contributing to cancer invasion and metastasis. According to current views on EMT in COPD airways may in addition be a crucial link between COPD itself and the development of lung cancer.

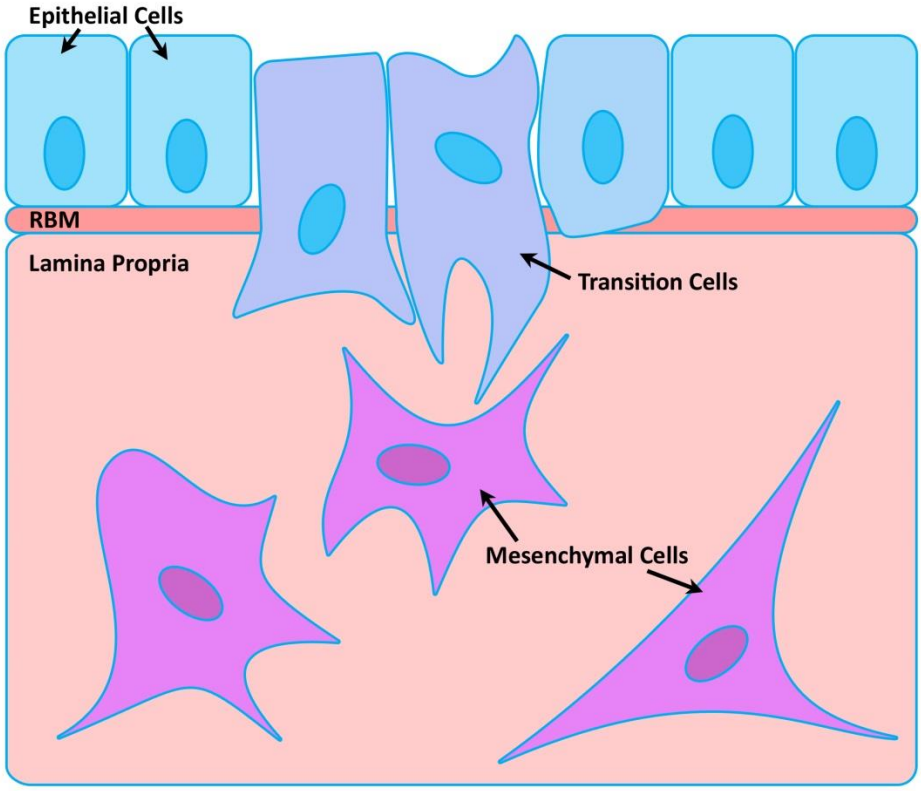

Figure 1.4 Epithelial-mesenchymal transition process.
RBM: Reticular basement membrane.

1.2b Airway component

Central/large airways (chronic bronchitis)

The diagnosis of chronic bronchitis was pioneered and measured by the pathologist Reid in 1954 (19). She measured the enlarged bronchial mucous gland layer and stated that chronic bronchitis is associated with inflammation involving the mucosal surface, submucosal glands, and gland ducts in smaller bronchi between 2 and 4mm in diameter (39).

Chronic bronchitis is essentially an inflammatory condition and can be a significant part of COPD. Excessive cigarette smoking is one of the most critical factors in causing bronchitis. Also, inhalation of dusts, fumes, chemicals like silica, iron, steel, asbestos, carbon, kaolin and less commonly the fumes of chlorine at work can cause pathological changes and inflammatory response in chronic bronchitis (40). When chronic bronchitis is associated with the chronic airflow limitation in COPD, it involves mucus gland hypertrophy, mucus hypersecretion, squamous metaplasia, loss of epithelial cilia, goblet cell hyperplasia, and infiltration of inflammatory cells including CD45, CD8, macrophages, and neutrophils in the epithelium of peripheral airways (please refer to Figure 4 in the Saetta *et al* paper) (41).

Although worsening of inflammation in bronchitis can contribute significantly to the progression of COPD, a number of longitudinal studies have found that its presence alone does not predict the airflow limitation of COPD (11, 42). Analysis of lung tissues over the

years has indicated that the changes in the small airways and the small airway wall remodelling can couple with the inflammatory cells in large airways to induce COPD (43).

Small airways (obstructive bronchiolitis)

Macklem and Mead were the first to introduce the resistance in small airways in 1967 (44). Soon after, Hogg and his colleagues suggested that small airway abnormalities can contribute significantly to airflow limitation in COPD (28, 39, 43, 45-49). There is an increased interest in small airway disease and some new insights have been gained over recent years on their contribution to the clinical expression of COPD.

Hogg's extensive study found that inflammation in small airways is an important feature of COPD pathology. However, interestingly he also showed that tissue remodelling in the small airways, including small airway wall fibrosis and obliteration, were the most important independent factors for the aetiology of COPD, rather than inflammation (please refer to Figure 1 in the Berge *et al* paper) (50). The exact mechanisms behind the small airway damage still remain obscure. Several possible mechanisms have been suggested. Chronic inflammation can play an integral role in stimulating fibrotic changes in the peripheral airways (50). The ongoing inflammation is responsible for an increased production of transforming growth factor beta (TGFβ). TGFβ is a fibrogenic multifunctional cytokine that is very important in the cell organization, development, proliferation, and immunology (51-53). Long term exposure to cigarette smoke itself can also cause increased production of TGFβ, pro-fibrotic growth factors such as connective tissue growth factor (CTGF), platelet-derived growth factors (PDGF) and TGFβ induced transcription factors such as Smad proteins (54). These changes can lead to altered extracellular matrix (ECM) structure of the airway wall in COPD subjects.

Lung parenchyma component (emphysema)

Hogg *et al* examined small airway remodelling and alveolar destruction in emphysema in COPD subjects using micro-computed tomography (micro-CT) (55). They investigated the number of small airways, their minimal cross-sectional lumen area, and lung parenchyma in four lungs removed from patients with very severe COPD and four unused donor lungs as control by using micro-CT scanning. They found a 10-fold reduction in the number and a 100-fold reduction in the minimal cross-sectional lumen area of the small airways in COPD lungs, both in areas with and without emphysematous destruction. These results suggest that the narrowing and obliteration of small airways begin in the COPD group prior to the onset of emphysematous destruction. This again implies the importance of small airways as targets for disease prevention and treatment.

Chronic inflammation caused by cigarette smoke plays a significant role in causing emphysema (56). The ongoing inflammation leads to destruction of airspace structure and disturbance of normal maintenance of alvelolar structure by mobilization of inflammatory

cells to the lungs and the release of potentially destructive cytokines (56). Inflammation also stimulates apoptosis in alveolar cells and there are good evidences that support the additional role of apoptosis in generating emphysema (56, 57). Consequently, these lung parenchymal destructions cause a reduced elastic recoil pressure that is available to push the air out of the lungs. This may also lead to dynamic airway collapse. These pathological changes in emphysema may eventually result in decreased ventilator function and hampers optimal airflow (58).

1.3 Epithelial-mesenchymal transition (EMT) in COPD

1.3a Centre of Research Excellence for Chronic Respiratory Disease (CRE) Breathe Well group work

In addition to the thickening and squamous metaplasia of the epithelium that are well described in COPD airways, CRE Breathe Well group recently highlighted changes in the Rbm of the epithelium, with fragmentation and 'cleft' formation, and increased cellularity in larger airway biopsies (1, 59). These changes are highly reminiscent of the classic descriptions of EMT (59, 60). Indeed, it is difficult to know what else such changes could represent, and they are very different from the well-established changes in adult asthma (61). Further studies on airway biopsies from COPD patients confirmed up-regulation of various proteins well established to be bio-markers of EMT. Thus, we observed cells staining positive for the expression of matrix metalloproteinase (MMP) -9, the proteolytic enzyme that is one of the strong associates of EMT, the fibroblast protein S100A4 (also called fibroblast-specific protein, FSP-1, one of the most commonly used EMT bio-markers), and the mesenchymal protein vimentin (59). These cells were present both in the basal epithelium (BE) and clefts in the Rbm, and were shown not to be macrophages, neutrophils, dendritic/Langerhans cells or lymphocytes infiltrating from below. They seem to be of epithelial origin as they double-stain for S100A4 and cytokeratin (an epithelial marker) (62). The epithelium was shown to be in an activated state, with cells stained highly positively for epidermal growth factor receptor (EGFR) (29). These histological features were all present in physiologically normal smokers, and in COPD ex-smokers, but were most marked in COPD current-smokers (63, 64). We also noted vessel changes, with hyper-vascularity of the Rbm and epithelium and hypo-vascularity in the LP, but these were evidently more smoking related than COPD related (65).

After CRE Breathe Well publications on larger airway biopsies, CRE and other different groups have shown that similar changes of EMT are also present in small airways (64, 66, 67), but preliminary results suggest that EMT in small airways is not accompanied by hyper-vascularity (64).

1.3b Other groups' work

The Milara *et al*. study also demonstrated that cigarette smoke extract (CSE) can induce EMT in primary human bronchial epithelial cells (HBECs) through modulating the TGFβ pathway and intracellular adenosine cyclic monophosphate (cAMP) levels *in vitro* (67). In a similar *in vitro* model, Wang *et al.* observed a significant correlation between urokinase plasminogen

activator receptor (uPAR) and vimentin expression indicating a potential uPAR-dependent signaling pathway for CSE-induced EMT(66). Another *in vitro* study by Câmara and Jarai demonstrated that EMT could be induced by TGFβ through the Smad2/3 pathway in primary human bronchial epithelial cells. The TGFβ stimulated EMT was enhanced by the presence of extracellular matrix (ECM) protein fibronectin and tumour necrosis factor α (TNFα) (68).

Interestingly, the non-neuronal cholinergic system is also getting remarkable attention recently in playing a possible role in inducing EMT in airway diseases. Acetylcholine (ACh), one of the principal neurotransmitters that is synthesised by certain neurons, is a key player in the nervous system. However, recent study has identified ACh and acetylcholine receptors (AChR) in many other non-neuronal cells and tissues, including airway epithelial cells (69). The use of anticholinergic therapy in COPD is widely used based on the parasympathetic activity that is increased in the airway inflammation (70). However, Gosens *et al*'s novel study also found that dysfunction of the non-neuronal cholinergic system of ACh can also play a significant role in the pathophysiology of COPD (71). Muscarinic acetylcholine receptors (mAChRs) are extensively expressed in the airways and are associated with airway remodelling, including airway smooth muscle thickening, differentiation, profound proliferation, collagen secretion, and fibroblast to myofibroblasts transition (71, 72). A recent study by Milara *et al in vitro* demonstrated that a new long-acting muscarinic receptor antagonist called aclidinium inhibits human lung fibroblast to myofibroblasts transition induced by carbachol, an analogue of ACh and TGF-β1 stimulation (73). Furthermore, they also reported that the non-neuronal cholinergic system is involved in cigarette smoke-induced lung fibroblast-to-myofibroblast transition that is inhibited by aclidinium (74). Another anticholinergic, tiotropium, is also reported to inhibit MMP production from lung fibroblasts induced by TGFβ through the suppression of Smad signalling and inhibiting protein phosphorylation (75). These evidences suggest the potential effects of non-neuronal cholinergic system in TGF-β pathway and its role in EMT. Yang *et al* is one of the first to explore the role of ACh and pathway involved in EMT in airway diseases (76). This study pointed towards a possible crosstalk between mAChR activation and TGFβ expression in stimulating EMT. ACh may function via M1 and M3 receptors in the airways through the Smad2/3 and ERK signalling pathways (76).

Despite the *in vitro* work looking at the pathways that can potentially drive EMT in human airways, the drivers and pathways of EMT *in vivo* in the airways of COPD patients still remain to be confirmed.

1.4 Definition of EMT

1.4a What is EMT?

Elizabeth Hay from Harvard University initially described a process she termed 'epithelial–mesenchymal transformation' in a model of chick embryo primitive streak formation (77). In time, the term 'transformation' has been replaced with 'transition', reflecting its possible reversibility in a two-way process (78). Recent interest in EMT stems less from its developmental importance, but more from emerging evidence of its involvement in promoting organ fibrosis (78), tumor formation and cancer metastasis (79). EMT is an example of what evolutionary biologists call 'exaptation': alteration in the function of a basic trait to provide new functions under new circumstances. Thus, insults to epithelial cells by cigarette smoke can activate EMT (67), changing cellular identity and promoting sustained tissue disruption that can potentially stimulate fibrosis, compromise tissue integrity and organ function (80) and/or enhance oncogenesis (78). Given this background, EMT has been classified into three subtypes based on the context (60). Type 1 EMT is associated with gastrulation and embryogenesis during organ formation (physiological). Type 2 EMT can also be a normal physiological process of tissue repair to generate fibroblasts in wound healing. However, it can result in organ destruction if it is persistent in the context of an ongoing pro-inflammatory insult. For example, the alveolar epithelial cells in idiopathic pulmonary fibrosis are morphologically abnormal, showing altered cytokeratin expression and producing ECM remodeling proteins such as MMPs. They have been shown to express mesenchymal markers in lung biopsies from idiopathic pulmonary fibrosis patients, and it has been proposed they contribute to fibrosis in vivo (81). Type 3 EMT is associated with epithelial tumors: both as a pro-tumor mechanism and also then subsequently used by epithelial tumors to invade and metastasize. This more sinister form of EMT Type 3 is associated with accompanying hyper-vascularity (1, 60, 65). In this context, it needs to be noted that epithelial tumors are very common and indeed make up 90% of human cancers, for example, breast, prostate, lung (airway), bowel, esophagus, stomach, pancreas etc., and EMT may be the unifying underlying pathological process which makes sense of this particularity (30-33, 79).

1.4b Potential EMT drivers in COPD

Epithelial 'stress', however caused, is thought to activate EMT, creating critical and self-perpetuating pro-fibrotic, pro-remodeling and pro-cancer events. These events are complex, involving potential activation of a number of signaling pathways, but converging on several prominent transcription factor families; some of these (e.g., Twist, Snail, Slug) are EMT specific while others (e.g., β-catenin and Smads) are somewhat less specific, but still potentially involved. Although there is no research data yet identifying the drivers involved in the process of driving EMT in COPD, the plausible pathways are reviewed below.

1.5 Transforming growth factor beta

TGFβ is one of the most important and sophisticated tissue and cell-regulatory networks and has been implicated in driving EMT (Figure 1.5) (82, 83), particularly the isoform TGFβ1. It may be a 'master switch' of fibrogenesis in many organs, including the lung (81, 84, 85). TGFβ1 has been one of the most widely studied cytokines/mediators of EMT (53).

1.5a Smads as transcription factors of TGFβ signaling

Studies on human alveolar and bronchial epithelial cell lines have shown that TGFβ1 can induce EMT via Smad2 activation (Figure 1.5) (86, 87). Evidence for a direct role for TGFβ in the effector end of EMT in the lung *in vivo* was given by the overexpression of active TGFβ1 in myofibroblasts in injured lungs, associated with EMT *in situ* (88). EMT in response to TGFβ1 ligand binding is thought to be mediated predominantly via Smad-transcription factors (82, 89).

Smads are classified into three subclasses, that is, receptor regulated Smads (R-Smads), common partner Smads and inhibitory Smads. Smad2 and Smad3 are R-Smads, activated by TGFβ Type I receptors. In contrast, Smad6 and Smad7 function as inhibitory Smads, while Smad4 serves as the common partner Smad in mammals, that is, it combines with R-Smads to activate them (90), and the complex translocates to the nucleus to act as transcription factors.
TGFβ transmits its signals through its serine-threonine kinase receptors, which upon activation are internalized into early endosomes where it associates with 'Smad anchor for receptor activation' which modulates the formation of complexes with Smad2 or Smad3 (81). The R-Smads are then phosphorylated by the receptor, which induces their association with the common partner Smad4 for translocation to the nucleus (Figure 1.5). In the nucleus, this Smad complex binds to promoter regions of target genes in further association with various other DNA-binding proteins (90).

Recent studies suggest that the majority of TGFβ1 target genes are controlled through Smad3-dependent transcriptional regulation (91). Overexpression of inhibitory Smad7 consistently blocks Smad3-dependent EMT *in vitro* and *in vivo* (92). Smad2 and/or Smad3 are also associated with EMT-related tumor progression models (93). However, it has not yet been investigated whether the Smad signaling pathway is active in COPD airways.

1.5b Alternative (non-Smad) pathways of TGFβ signaling

Smad-independent signaling has also been implicated in EMT (89), although less is known about it or its relevance. Non-Smad-dependent pathways implicated in TGFβ-elicited EMT include activation of extracellular signal-regulated kinases (Erk)/mitogen-activated protein kinases (MAPK), Rho GTPases and the phosphatidylinositol-3-kinase /Akt pathways (Figure 1.5) (81, 82), although these are less established compared to Smad dependent pathways and have been reported mainly in *in vitro* studies (94-96). However, MAPKs, originally called Erks, are required for the induction of cell motility and disassembly of cell adheren junctions after TGFβ stimulation. The TGFβ-stimulated Erk signal also regulates transcription of genes which are known to function in the modulation of integrin-based cell matrix adhesion to promote cell motility (97). Erks regulate target gene transcription through activating its many

downstream transcription factors, such as ELK1 (a transcription activator), to influence EMT (97, 98).

To add to this complexity, there may be significant crosstalk between the Smad-dependent and Smad-independent pathways, with non-Smad proteins modulating Smad activity and vice versa. But the Smad independent pathways have not yet been investigated in EMT in the airways.

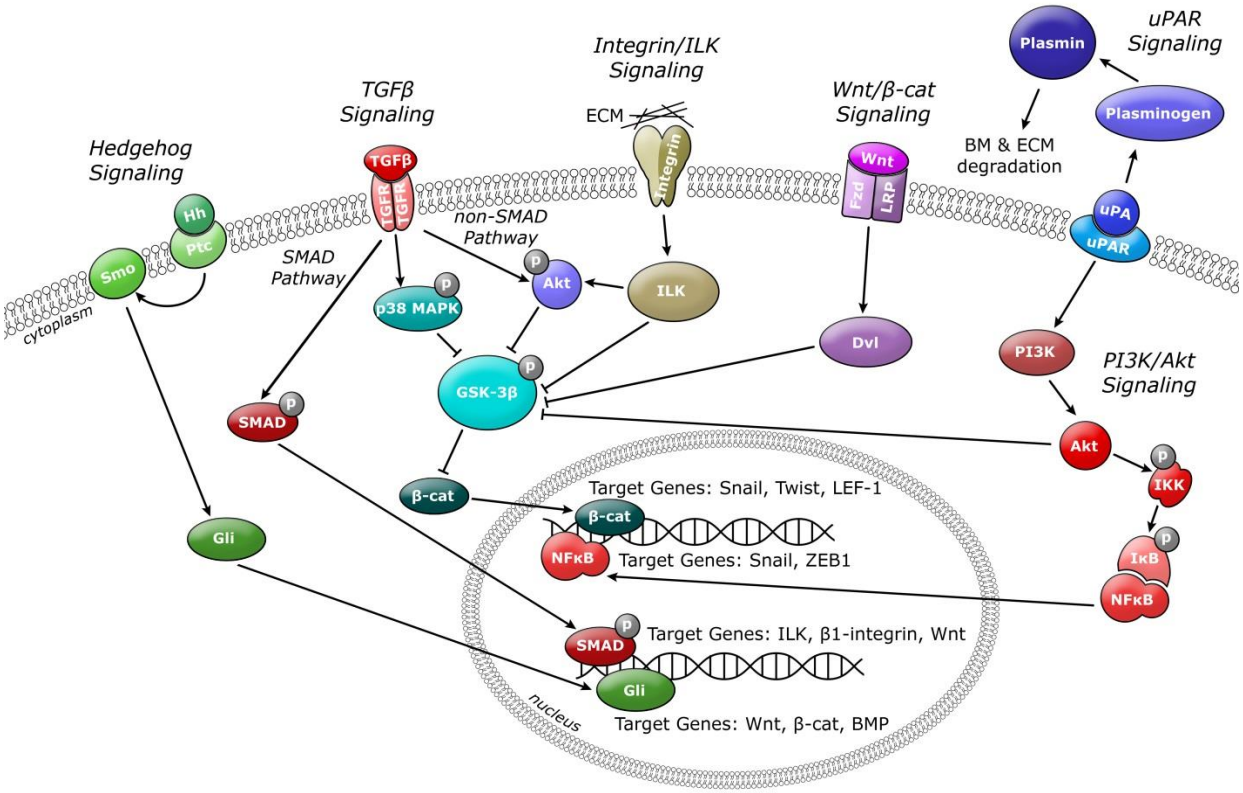

Figure 1.5. A simplified schematic diagram showing the major potential drivers of epithelial–mesenchymal transition. These pathways are complex and inextricably interconnected. The Smad pathway for TGFb signaling acts through formation of a complex between Smad2/3 and Smad4. The complex then moves to the nucleus and stimulates transcription of their target genes. Sharp arrows denote activation/upregulation and blunt arrows denote inhibition/downregulation. BM: Basement membrane; BMP: Bone morphogenic protein; DVL: Disheveled; ECM: Extracellular matrix; Fzd: Frizzled receptors; Gli: Glioma-associated oncogene family of transcription factors; GSK-3b: Glycogen synthase kinase; Hh: Hedgehog; PI3K: Phosphatidylinositol-3-kinase; ILK: Integrin-linked kinase; LEF-1: Lymphoid-enhancer-binding factor-1; LRP: Low-density lipoprotein receptor-related protein; p38 MAPK: Mitogen activated protein kinase; Ptc: Patched receptor for Hh signaling; SMO: Smoothened; TGFβ: Transforming growth factor beta; uPAR: Urokinase plasminogen activator receptor. Adapted from (83).

1.6 Other potentially primary transcription factor families

1.6a Snail1, Snail2 (Slug), Twist in EMT

There is evidence for a direct link between TGFb1 signaling and induction of Snail/Slug expression, thought of as specific 'primary' transcription factors for EMT induction, acting through β-catenin release (99-101). There is evidence that the Snail family transcription factors promote EMT through β –catenin transcription encouraging its accumulation and availability to act as a pro-EMT transcription factor (102). Furthermore, Snail and Slug are strong epithelial cadherin (E-cadherin) repressors implicated in inducing EMT through accumulation of β-catenin by releasing it from its role in inter-cell-adhesion complexes. These transcription factors are differentially expressed in different tissue contexts (81), and whether one or both are involved in COPD airway disease has not yet been investigated.

Twist is another transcription factor regarded as a 'master' regulator of embryonic morphogenesis and is also thought to play an essential role in up-regulating EMT, at least in metastatic and invasive carcinomas (103). Again, it seems to work at the levels of E-cadherin suppression and β-catenin accumulation. Its potential role in airway EMT deserves attention.

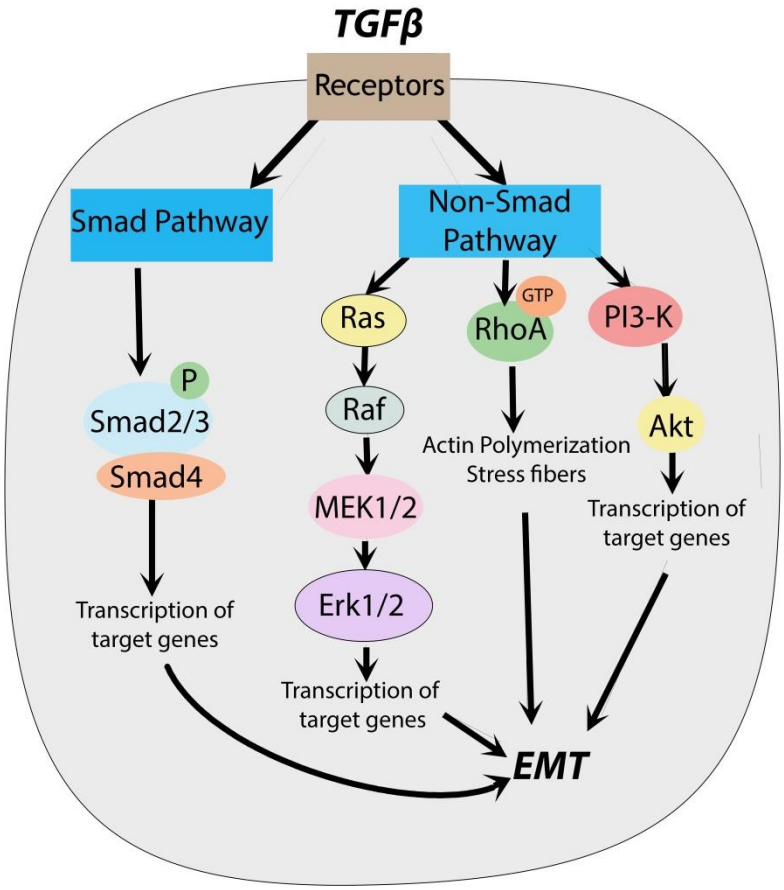

Figure 1.6. Smad and non-Smad pathways in transforming growth factor β-activated epithelial–mesenchymal transition. EMT: Epithelial-mesenchymal transition; PI3-K: Phosphatidylinositol 3-kinase.

1.7 Wnt pathway in EMT

The name Wnt is a combination of Wg (Wingless) and int (integration) genes and stands for Wingless-related integration site (104). Wnt signaling was originally identified in playing a role in carcinogenesis, but the signaling pathway since then has been well characterized in embryonic development, including cell fate specification, cell proliferation, differentiation and epithelial–mesenchymal interactions (105, 106). Wnt ligands are a large family of secreted glycoproteins and highly hydrophobic. In vertebrates, there are 19 different Wnt proteins whose expression is regulated during development. Wnt ligands bind and transmit their signal across the plasma membrane through binding to both Frizzled receptors and low-density lipoprotein receptor-related protein (LRP) (107).

1.7a Role of Wnt & β-catenin

Activation of EMT is classically characterized by decreased production of E-cadherin, which is part of the adheren molecular aggregates responsible for epithelial cell–cell adherence. A second component of adheren complexes is β-catenin, which plays an integral part in adheren junctions by linking E-cadherin to the cytoskeleton. When E-cadherin is less available, for example, if its nuclear transcription is inhibited, the adheren complex breaks up and free cytosolic β-catenin may accumulate (107). β-catenin is known to be a key player in the Wnt pathway and has also been implicated as a driver in EMT, by itself potentially acting as a transcription factor or transcriptional co-activator of other transcription factors (108). This occurs when cytosolic β-catenin accumulates. However, free cytosolic β-catenin is normally kept suppressed and inactive in epithelial cells through a strategic enzyme, glycogen synthase kinase-3β (GSK-3β), leading to its phosphorylation and subsequent ubiquitination and proteosomal degradation.

Wnt ligand activation of its receptor complex leads to phosphorylation of LRP, again by GSK-3β, resulting in recruitment of the cytosolic proteins Dishevelled and Axin. The formation of Frizzled - Dishevelled and LRP-Axincomplexes results in active release of β-catenin from E-cadherin complexes into the cytoplasm and at the same time inhibits the β-catenin phosphorylation by GSK-3β. The cytoplasmic accumulation of b-catenin is therefore complex and has several causes, but this accumulation enables β-catenin to move into the nucleus to act as an important pro-EMT nuclear transcription factor (Figure 1.5) (102, 107-109). It has also been suggested that the formation of complexes between the members of Snail family of transcription factors, β-catenin and another transcription factor known as lymphoid enhancer factor can induce EMT under TGFβ stimulation (102). The potential role of crosstalk between TGFβ and Wnt signaling pathways in mediating EMT in pathological events, especially in our case COPD, remains to be determined.

1.8 Other pathways implicated in EMT

1.8a Hedgehog pathway

Another important signaling pathway described as inducing EMT is Hedgehog (Hh) signaling (Figure 1.5)**,** which was initially discovered in Drosophila by Wieschaus and Volhard (110). Hh is a major regulator of cell proliferation, differentiation and tissue polarity. The Hh family consists of three Hh proteins, including Sonic Hedgehog, Desert Hedgehog and Indian Hedgehog (107). Binding of Hh ligands to their receptors causes activation of a family of transcriptional factors through complex cascades. This leads to the up-regulation of Wnt protein, β-catenin and bone morphogenic protein accumulation in the cytoplasm.

Wnt and Hh signaling are both mediated by the G-protein coupled Frizzled receptors, and both pathways prevent phosphorylation-dependent proteolysis of β-catenin. In addition, the molecules involved in Wnt signaling such as GSK-3β also regulate Hh signaling, suggesting crosstalk between the two potential pathways. Emerging evidence suggests the activation of Hh signaling in numerous human cancers, including lung cancer (110). The available literature on Wnt and Hh signaling shows that these pathways can be crucial for driving cancer cells toward aggressiveness, but relevance to COPD has not been investigated.

1.8b Integrin-linked kinase pathway

The important potential role of integrin-linked kinase (ILK) signaling (Figure 1.5) in EMT and associated tumor progression has been described frequently over the last few years. ILK acts as a growth factor signaling protein and regulates a diversity of processes such as proliferation, apoptosis, survival, invasion and angiogenesis (111). Accumulating evidence suggests that in human malignancies, ILK activity is overexpressed. A recent study on the role of ILK in lung cancer aggressiveness showed over expression of ILK which promoted cell invasion, migration and metastasis, associated with acquisition of an EMT phenotype (112). ILK, perhaps in combination with TGFβ, induces the de novo expression of several integrins, such as a5β1, avβ3 and avβ6, which enhance the migration and invasion of carcinoma cells, particularly in conjunction with MMPs and fibronectin (113). ILK, TGFβ and Wnt signals (Figure 1.5) are interconnected and converge at the activation of a number of transcription factors which leads to the activation of EMT transcriptional programs, but has not been studied in COPD airways.

1.8c uPAR pathway

A recent study by Wang et al. showed that uPAR signaling can also play a role in EMT (66). Urokinase was originally isolated from human urine, but can also be present in several other locations including the ECM. The main physiological substrate for urokinase plasminogen activator (uPA) is plasminogen. When uPA, a serine protease, binds to uPAR, plasminogen is activated to form plasmin (Figure 1.5)**.** Activation of plasmin triggers a proteolytic cascade that can participate in remodeling of ECM, degrading components of BM and hence, allowing cells to move across and through these barriers (66, 114). Binding of uPA to uPAR can induce EMT through activating a number of cell-signaling factors, including

phosphatidylinositol 3-kinase (PI3k), Src family kinases, Akt, ERK/MAPK and myosin light chain kinase (114-116). Among them, only the PI3k/Akt pathway has been studied a little in uPAR signaling in EMT. Activation of PI3k signaling catalyses the formation of phosphatidylinositol 3,4,5-phosphate,which can influence cell morphology through its effect on actin cytoskeleton reorganization and migration (114). Another mechanism by which PI3k may also be involved is through the activation of Akt, which can promote cell invasion (114) and regulate the activity of several transcription factors, including NFkB (nuclear factor kappa B) that binds to the DNA sequence and can directly/indirectly induce EMT, sometimes through intermediate transcription factors Snail or ZEB-1/2 (Figure 1.5)) (117).

1.9 Evidence of EMT drivers in human airways

In the lungs, a significant correlation was found between the increased expression of TGFβ and the increased thickness of the BM and the increased number of fibroblasts in mucosal biopsies in both asthma and chronic bronchitis (51). In this study, TGFβ was localized to both structural cells such as epithelial cells and fibroblasts as well as to eosinophils (51). The expression of TGFβ1 mRNA in small airway epithelium from smokers and patients with COPD was significantly higher than in non-smoker controls (84). Furthermore, among smokers with COPD, the TGFβ1 mRNA levels correlated positively with the extent of smoking history (pack-years) and the degree of small airway obstruction (84). Our group showed an increased expression of vessel-associated TGFβ in the bronchial RBM in COPD but also in normal smokers (118). We did not find an increase in TGFβ in the epithelium in large airway biopsies, so the story of how TGFβ may be operating in COPD needs to be clarified.

Apart from TGFβ, there has been little work in airway tissue on potential drivers of EMT. Although Wang *et al* showed uPAR signaling pathway to be present in small airway tissue from COPD subjects (66), there has not been adequate focus on other potential drivers of EMT. There is a great possibility that different signaling pathways may be participating in the progression of COPD disease at different stages and in anatomically different sites, for example, large versus small airways. A lot more research work needs to occur.

1.9a Vessel-associated TGFβ activity in COPD-smokers

As I have stated before, TGFβ is a cytokine with plethora of functions including angiogenesis, in numerous cells and tissues including epithelial, endothelial, hematopoietic, neuronal cells and connective tissue. Moreover, platelets and megakaryocytes are an abundant source of TGFβ1 in humans (119). Of the several functions of TGFβ, stimulation of angiogenesis should be highlighted as it can be associated with human disease, particularly cancer. TGFβ can act as a direct/indirect angiogenic factor promoting angiogenesis through the downstream induction of other cytokines, such as vascular endothelial growth factor (VEGF), that is a potent regulator of angiogenesis in various malignancies (119). The study published by the Kranenburg and colleagues has suggested that bronchial vascular changes may occur in COPD, they did this by demonstrating the VEGF expression in vascular and airway smooth muscle cells, epithelial cells, and macrophages using immunohistochemistry (120). On the other hand, the endothelial cells only showed VEGF receptor expression, but not VEGF, indicating the endothelial cells being effector cells for VEGF to act on rather than an important autocrine source (120). A number of factors relevant to COPD have been shown

to increase VEGF expression and release, these include cigarette smoke (121) and cytokines such as TGFβ (122). In addition, TGFβ receptors are suggested to play a key role in the pathogenesis of COPD through their Smad pathways (39). Hence, there could be an important link between Smad expression through the angiogenic effects of TGFβ in COPD as well as in lung cancer that needs to be addressed. My study on Smads predominantly focuses on this scenario.

The study by our group previously found that in smokers with COPD there was a suggestion that the increase in blood vessels in the Rbm was related to both VEGF and TGFβ1 (118). This relationship was not evident in the COPD ex-smokers or normal lung function smokers group with only the TGFβ increase in Rbm vessels implying that in the COPD-smokers group the vascularity is driven by both TGFβ and VEGF whereas in the other two groups it is only related to TGFβ (118). EMT and fibrosis in response to TGFβ is stimulated predominantly through Smad dependent (mainly Smad2 and Smad3) pathways (81). Smads are intracellular proteins that act as transcription factors that transduce extracellular signals from TGFβ to the nucleus where they activate gene transcription (123). The name SMAD is a portmanteau of the two proteins: the Drosophila protein, *mothers against decapentaplegic* (MAD) and the *Caenorhabditis elegans* protein SMA (from gene sma) (124).

In the Smad regulated pathway, TGF-β1 signals are transduced by transmembrane serine/threonine kinase type II and type I receptors. The receptors are internalised into early endosomes where Smad anchor for receptor activation (SARA) modulates formation of complexes with Smad2 or Smad3. There is another inhibitory type of Smad, Smad7, which can inhibit TGF-β signaling through inhibition of TGF-β receptor I phosphorylation (125). When there is no inhibition, Smad2 and Smad3 are then phosphorylated at serine residues by the type I receptor. Phosphorylation induces their association with Smad4 and translocation to the nucleus where they stimulate TGFβ -responsive gene transcription (81).

Originally, it was found that TGFβ gene transcription can endogenously produce TGFβ that then acts as an autocrine negative growth regulator (126). Hence, it was hypothesised that it may inhibit proliferation and consequently, may act as an inhibitor of tumor progression (127). Conversely, some studies have found that TGFβ can potentially stimulate proliferation (128, 129). Therefore, this discrepancy may possibly be explained by the concentration of TGFβ within the cell, with low endogenous concentration of TGFβ resulting in proliferation and high endogenous concentration inducing growth arrest (127). In this case, the role of Smads as transcription factors of the TGFβ pathway may become important. Low intercellular TGFβ concentration may activate the receptors and thereby allow the Smad pathway to be utilised leading to more TGFβ release and proliferation of the cell. Because of this dual role of TGFβ as a pro-oncogenic factor in addition to its tumor suppressor role, members of the TGFβ signaling pathway, such as Smads are considered as predictive biomarkers for disease progression, particularly tumorigenesis (127). An important aspect of TGFβ is its ability to induce EMT and numerous studies are currently investigating EMT markers and its relevance in identifying airway pathology in COPD (62, 66, 67).

1.10 Aim

The aim of this study was to study the immunostaining of the key transcription factor, phosphorylated Smad2/3 (pSmad2/3) in order to study TGFβ signaling, in the COPD airways, epithelium and underlying tissues.

1.11 Rationale of study

Transforming growth factor beta (TGFβ) is a multifunctional cytokine that is present in many tissues and cells in the human body (53, 82, 87, 92, 109, 130-132). There are only limited data available on its role in COPD. It has been shown that TGFβ1 immunostaining in COPD airways were increased in the bronchial reticular basement membrane in smokers, and correlated with an increased in vascularity, especially in those who are current smokers (118). One important manifestation of EMT activity through TGFβ pathway involves up-regulation of specific key transcription factors, such as Smads, particularly phosphorylated Smads (92, 132, 133). Hence, immunostaining of the pSmad2/3, which is most commonly seen, was measured and analysed to determine the possible TGFβ pathway in COPD airways and their involvement in pathogenesis.

Chapter 2 – Materials and Methods

2.1 Subjects and study design

Informed consent was received from all subjects. Two main studies were designed to examine the immunostaining of pSmad2/3, the first one was cross-sectional and the second one was longitudinal.

The cross-sectional study involved an analysis of pSmad2/3 immunostaining in COPD subjects and smokers against controls, using lung biopsies obtained at fiberoptic bronchoscopy. The study was approved by the Alfred Hospital in Melbourne and the Royal Hobart Hospital (RHH) Ethics Committees and participants were recruited by advertisement in local newspapers and placement of posters in the clinic waiting areas in the hospitals and on the notice boards. Tissue collection was started in Melbourne, but was continued in Hobart when Professor Walters moved his team.

Endobronchial biopsies from 15 healthy non-smokers as controls (NC), 13 smokers with normal lung function (NLFS), 15 COPD current-smokers (COPD-CS) and 14 COPD ex-smokers (COPD-ES) were analysed for the study. Any participant with a history of any other respiratory disorder was excluded. They all were aged above 50. Their cigarette smoking histories were recorded as pack years (by multiplying the number of pack of cigarettes smoked per day with the number of years the person has smoked, divided by 20). Their lung function results were measured as percentage predicted forced expiratory volume in 1 second (FEV_1) and ratio of FEV_1 to forced vital capacity (FVC) as percentage.

Finally, a longitudinal study was performed in matched COPD subjects where Smad expression was measured before and after the inhaled corticosteroid (ICS) fluticasone propionate (0.5mg/twice daily) or placebo therapy for 6 months (2:1 ratio of ICS vs placebo), as part of a study of airway remodelling in COPD and response to corticosteroid. For the second time point in the original study there were 11 treated and 4 placebo from the COPD current cohort, and there were 8 treated and 6 placebo from the COPD ex cohort. However, for this component of the study for the COPD current smokers there were only material from 7 of the subjects of which 6 were treated with ICS and 1 was from the placebo arm, for the COPD ex-smokers there were only materials from 5 of the subjects of which 3 were treated with ICS and 2 were treated with placebo.

2.2 Statistics

A Shapiro-Wilk normality test was performed in SPSS and indicated all 4 groups significantly deviated from normal distribution. Skewed histograms and a normal Q-Q plot also showed non-symmetric distribution. The Kruskal-Wallis H test in SPSS was then used to determine if there were statistically significant differences between the different groups. Based on the output of the Kruskal test, a Tukey post hoc test was used to determine where the differences lie between the groups. All analyses were performed using SPSS statistics. Two-tailed p values <0.05 were considered as significant.

2.3 Bronchoscopy

The laboratory facilities used for this research project included standard histology labortory equipment, a Dako immunostainer (Denmark), and computerised image analysis using Leica DM2500 light microscope (Switzerland) and Image Pro-Plus 7 software (Media Cybernetics-the USA) in medical science 1 (MS1) building at University of Tasmania (UTAS) as part of the Centre of Research Excellence (CRE) Breathe Well infrastructure.

Subjects fasted overnight before the bronchoscopy. After the subjects were sedated with intravenous administration of midazolam (5-10mg) and fentanyl (50-100microgram) and topical lignocaine (200-400mg) to throat, larynx, and airways, bronchoscopy was conducted by respiratory physicians from the Department of Respiratory medicine in both hospitals. Prior to bronchoscopy, subjects were pre-medicated with nebulised salbutamol (5mg) approximately 15-30 minutes before the bronchoscopic examination. This procedure was done using a flexible fiberoptic bronchoscopy called Olympus Video-bronchoscope (Japan) instrument. Eight endobronchial biopsies (EBB) were taken from subcarinae of uninvolved contralateral bronchus of each subject using alligator forceps inserted parallel to bronchoscope. Blood pressure, pulse rate, and saturation of arterial oxygen were monitored during the procedure. Saline solutions were used to wash alligator forceps after each biopsy.

2.4 Processing of biopsies

4 biopsies were taken for each subject for paraffin (Sigma-Aldrich, Australia) embedding in 4 % buffered formalin supplied by the RHH. They were fixed at room temperature (RT) for 2 hours and then placed in 50% alcohol overnight or over the weekend if taken on a Friday. Biopsies were placed between two half sheets of “slide insert paper” in cassette with foam on either side. This makes biopsies easy to find prior to embedding. Cassettes were then placed in the automated processor Leica ASP200S as shown in Figure 1 and they were processes using xylene (Recochem Inc Australia), and 100% ethanol (Sigma-Aldrich, Australia) followed by 95% then 70%.

Figure 2.1: Automated Processor Leica ASP200S

Once the above processing was complete, the retort was drained and cassettes were removed to embedding centre (Figure 2.2) that was preheated to melt embedding wax and heat cassette holding chamber half an hour prior to the processor completing its cycle. Cooling plate, fume extractor and lights were switched on. A single biopsy was placed in a small steel mould. While using small moulds to fill with hot paraffin wax, a pair of forceps was used to hold biopsy in centre of mould and mould was moved onto small cooling plate on embedding centre. Biopsy was quickly and gently tamped and then labelled cassette was placed (A, B, C or D, initials, date of birth and reception date) on top of mould and filled with hot wax. Mould was moved onto large cooling plate and allowed to cool for half an hour prior to removing mould from embedded biopsy. Excess wax was removed from edges of biopsy by using heating plate for this purpose. Prior to cutting for Haematoxylin and Eosin (H&E), paraffin embedded tissue blocks were allowed to cool overnight before being stored at room temperature.

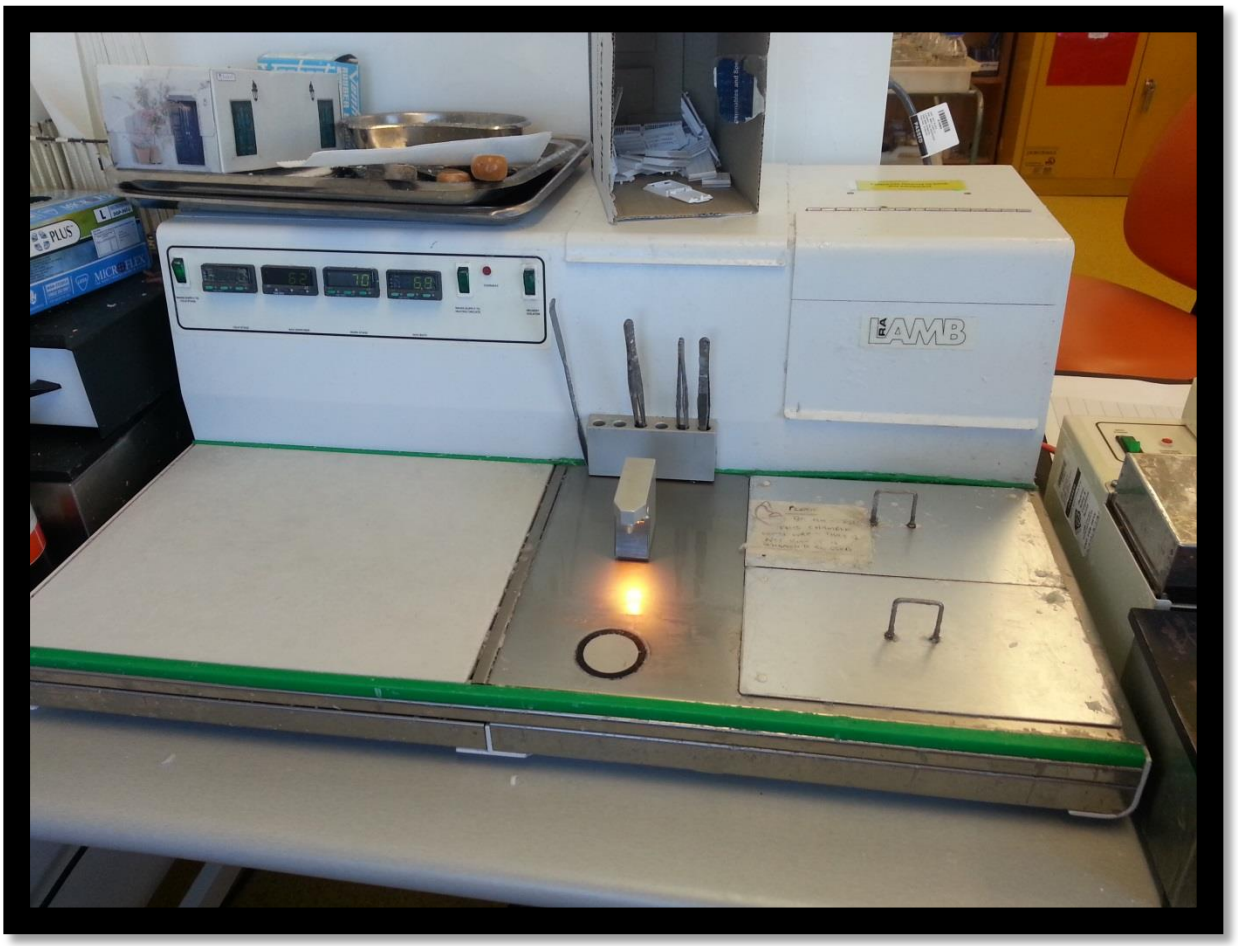

Figure 2.2: RA Lamb Embedding Centre

2.5 Sectioning of paraffin-embedded tissue blocks:

Paraffin-embedded tissue blocks of biopsies were effaced using the Leica RM2255 microtome (Leica Microsystems, Germany) shown in Figure 2.3. Then paraffin blocks were sectioned at 3.5 microns either after cooling in –20 degree freezer or on ice blocks for 5-10 minutes to assist with sectioning using the same microtome. Cut sections were transferred onto a deionised water bath containing one drop of Tween 20 (product code - ICN 103168) (to allow sections to unfold and spread out) at approximately 50°C. Two cut sections were picked up and mounted on each slide separated by 40-50 microns on Dako "IHC" (brand name) charged slides. Prepared slides were dried overnight at 37°C in incubator.

Figure 2.3: Leica RM2255 Microtome

2.6 Haematoxylin

Reagents used in haematoxylin stainingprocedure are listed in the Table 2.2 below Mounted tissue sections were de-waxed in two changes of xylene each for 5 minutes and then hydrated to water in descending grades of ethanol starting from 100% followed by 95% and 70% for two minutes in each change. A fume cabinet was used to do the steps. Then tissue sections were rinsed well under running tap water for two minutes.

Table 2.1: Reagents

Reagents	**Supplier**
Mayer's Haematoxylin	Australian Biostain P/L
Ammonia solution	BDH Chemicals Australia
Dako mounting medium	Dako

Tissue sections were then placed in Mayer's haematoxylin for five minutes to elaborate nuclei after which the sections were rinsed in running water to remove excess haematoxylin solution. Tissue sections were then placed in approximately 400ml of water mixed with 8 drops of ammonia solution for 30 seconds and later rinsed in running water. Tissue sections were checked under microscope to ensure nuclei were sufficiently stained. After that the sections were dehydrated in ascending grades of ethanol starting at 95% ethanol followed by two changes of 100% ethanol each for three minutes. Sections were cleared off ethanol using two changes of xylene for two minutes in each change. Tissue sections were then coverslipped with Dako cover glass 24 × 50 mm using Dako coverslipper. Slides stained for haematoxylin were used as the basis for selection of slides for immunostaining.

2.7 Immunostaining

Reagents used in immunostaining are listed in the Table 2.3. Heat-induced antigen retrieval solution was used as described in the specimen preparation and heat-induced antigen retrieval section. This was the EnVision FLEX solutions and target retrieval solutions intended for use in manual autoclave technique and the Dako PT Link equipment. All tissue specimens were treated with diluted 3% hydrogen peroxide (H_2O_2) for 20 minutes to block endogenous peroxidase activity.

Table 2.2: Reagents

Reagents and chemicals	Supplier
EnVision FLEX Target Retrieval Solution - Low pH (50x)	Dako Denmark
30% H_2O_2 diluted to 3% in de-ionised Water (H_2O)	Merck Victoria
EnVision FLEX Antibody diluent	Dako Denmark
EnVision Plus Anti-rabbit	Dako Denmark
TRIS Buffer	May & Baker
DAB	Dako
Anti-pSmad2/3 (Primary Ab)	Santa Cruz

- **Buffers**

0.05M Trishydroxy-methyl-amino-methane-hydrochloric acid (TRIS-HCl) saline buffer at pH 7.6 was used for the rinsing step of immunohistochemistry. This was prepared using reagents listed in the Table 2.4 below.

Table 2.3: Buffers solution

Reagents	Supplier
Trishydroxy-methyl-amino-methane (TRIS)	MP Biochemicals, LLC
Sodium chloride	Biolab (Aust) Limited
EMSURE Hydrochloric acid 32% for analysis	Merck KGaA Germany
Tween 20	ICN Biochemicals, Inc.

A stock solution of 0.5M Tris-HCl Saline Buffer pH 7.6 with Tween 20 was made from 60.56g of trishydroxy-methyl-amino-methane (TRIS) dissolved in 800ml de-ionised water, 90g of Sodium Chloride (NaCl) was added and dissolved in this solution. The pH of the solution was adjusted to 7.6 using concentrate hydrochloric acid (HCl) and 5ml of Tween 20 was added to the solution. The solution was then transferred to a volumetric flask and made up to 1L with distilled water. The stock solution of 1L was then made up to 10L with distilled water to a working solution (in the Dako Autostainer container) of 0.05M Tris-HCl saline buffer pH 7.6.

- **Primary antibody**

Primary antibody used for the purpose of immunohistochemistry (IHC) is listed in the Table 2.5 below.

Table 2.4: Primary antibody

Antibody	Type	Clone	Isotype	Company/ supplier	Concentration (fresh)
Anti-human pSmad2/3	Polyclonal rabbit	-	-	Santa Cruz	1/100 60min RT

- **Secondary link reagents and detection systems**

The EnVision+ system utilises a polymer-based immunohistochemical method with multiple antibodies on a polymer backbone and conjugated horseradish peroxidase (HRP) as depicted in the Figure 2.4 (134).

Table 2.5: Secondary link reagent and detection

Reagents	Supplier
EnVision+ System-HRP Labelled Polymer Anti-rabbit	Dako North America

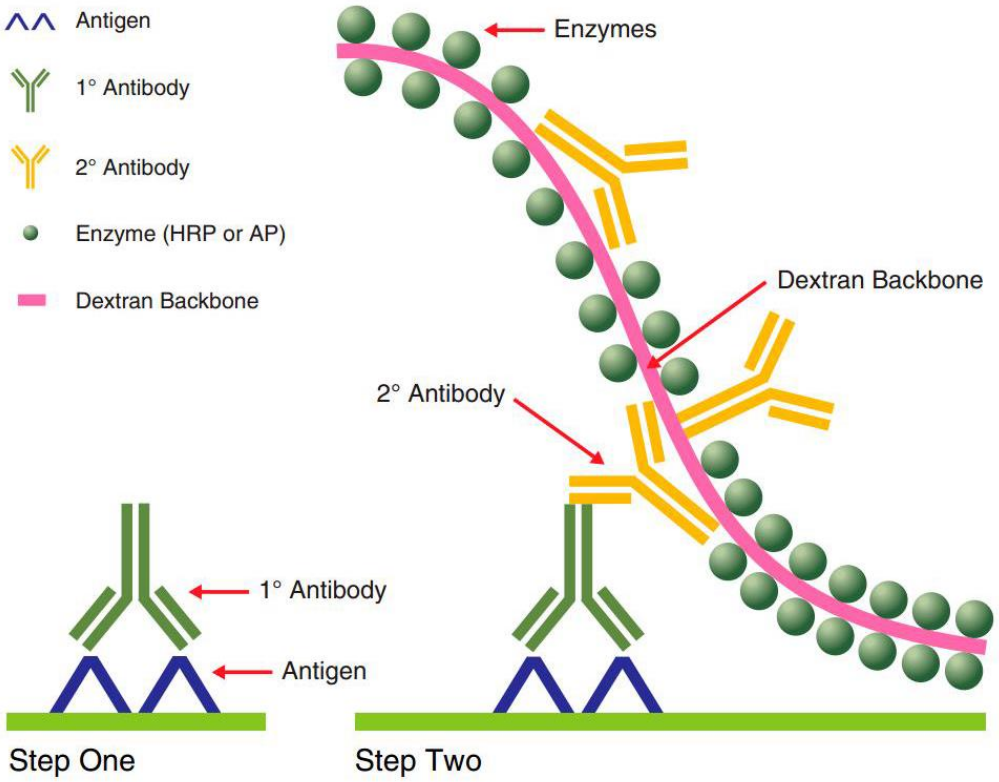

Figure 2.4: Labelled polymer horse-radish peroxidase system

- **Visualisation**

The chromogens used to enable visualisation in this study are listed in Table 2.7 below.

Table 2.6: Visualisation reagents

Reagents	Supplier
Liquid 3,3' Diaminobenzidine tetrahydrochloride (DAB) with substrate chromogen system	Dako North America

2.8 Specimen preparation and heat-induced antigen retrieval

Tissue samples underwent preparatory steps prior to immunostaining. Selected tissue sections were dried in an oven overnight at 37°C. Tissue samples were either treated for antigen retrieval using the Russell Hobbs pressure cooker or the Dako PT Link heat retrieval equipment. Methods for specimen preparation are described in the following section.

2.9 Autoclave using Russell Hobbs pressure cooker

Test slides that would undergo manual pre-treatment procedure using autoclave techniques were dewaxed and hydrated to water. Tissue samples that have been rinsed in running tap water for 2 minutes were then placed in a plastic container containing approximately 500mL of EnVision flex target retrieval solution low pH (Dako). Deionised water (500ml) was poured into the chamber of a Russell Hobbs pressure cooker as shown in the Figure 5, and the plastic container containing the test slides was placed in the pressure cooker. A plastic lid was loosely placed on the plastic container and the lid of the pressure cooker was secured. The pressure cooker was set to maximum heat for 6 minutes after which the dial was reduced to about 6.5 units for another 14 minutes just as the pressure cooker began to expel steam. The pressure cooker was then switched off and allowed to cool. The pressure cooker cover could only be removed once pressure inside has reduced. Test slides were then removed from the pressure cooker in the plastic container using a heat protective glove and allowed to cool below 35°C and then removed from the heat retrieval solution and rinsed in running tap water for 2 minutes. Test slides were then ready to be labelled and mounted onto the Dako Autostainer Plus as shown in Figure 2.7.

Figure 2.5: Russell Hobbs pressure cooker

2.10 Dako Pretreatment (PT) Link

Test slides pre-treated using the Dako PT Link equipment (Figure 2.6) for heat-induced epitope retrieval were de-waxed and hydrated to water as per the autoclave technique. EnVision FLEX Target Retrieval Solution low pH (Catalogue no. K8005, Dako, Denmark) (30mL) was poured into a tank in the Dako PT Link and the solution was made up to 1500mL with deionised water to give a dilution factor of 1 in 50. The tank was then preheated to 65°C. Labelled slides were then mounted onto a rack and placed inside the preheated tank. The Dako PT Link was programmed and the tank was heated to 97°C for 30 minutes after which it was cooled down back to 65°C. After the cycle has completed, rack containing slides were quickly and carefully removed from the tank and dipped into a PT Link rinse station that contained TRIS buffer pH 7.4 for 2 minutes as part of a quick-dip procedure. Test slides were then ready to be mounted onto the Dako Autostainer Plus as shown in Figure 2.7

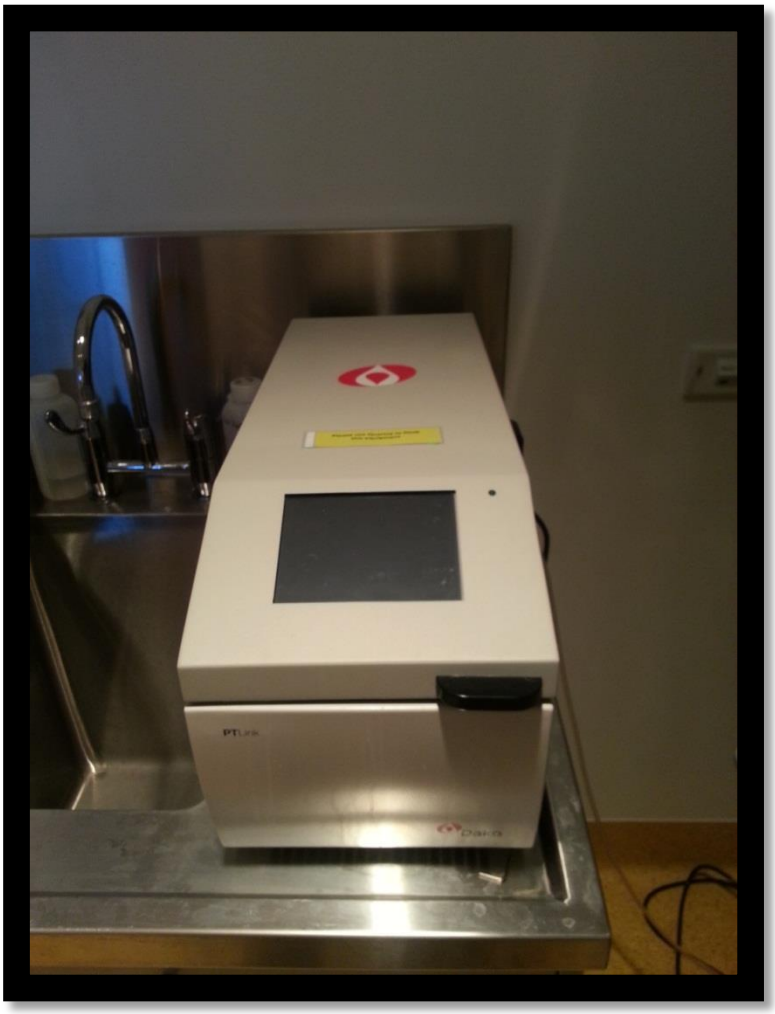

Figure 2.6: Dako PT Link

2.11 Immunostaining protocol

Immunostaining protocols based on specifications of primary antibody as described above were programmed into the Dako Autostainer Plus software prior to immunostaining. Slide identification information was entered onto the 'Slide Information' window. Abbreviations for the primary antibody used along with its dilution factors and relevant optimised conditions (eg. use of PT Link, high or low pH pre-treatment condition and use of protein block) were keyed into data entry field labelled 'Slide ID'. Participant's unique identifying number, an indication of endobronchial biopsy (BB) followed by an alphabetical sequence indicating the tissue block it was cut from were keyed into data entry field labelled 'Case#'. The Respiratory Research Group was labelled as the Doctor for all cases to allow data recovery in the future. The figure '1' was keyed into data entry field labelled '#Slides' indicating data entered were for one prepared slide. The entries were checked once again and entries were confirmed by clicking the button 'Finish Entry' to give an output programme.

Figure 2.7: Dako Autostainer Plus

Immunostaining protocols were programed into the Dako Autostainer Plus software. Treatment with endogenous enzyme blocks, primary antibodies, secondary link reagents and substrate as shown in table 6, as well as rinsing steps were entered into the program. Adhesive slide labels were then printed from the Dako Seymour Glass Label Printer. Prepared slides were then labelled prior to specimen preparation methods.

At the start of immunostaining protocols utilising the autostainer (and after heat retrieval), tissue samples were pre-rinsed with TRIS-HCl saline buffer. The visualisation system utilised in all immunostaining protocols in this study was horseradish peroxidase (HRP) using the Dako Envision+ system. As such, all slides were treated with 3% H_2O_2 for 20 minutes to block endogenous peroxidase activity in tissue samples and eliminate potential background staining. Tissue samples were again rinsed with TRIS-HCl saline buffer.

Tissue samples were then treated with specified primary antibody at optimised dilution factor (1/100) and incubated in the humidified staining chamber at appropriate incubation time i.e. 60 minutes (room temperature were set at 22°C and humidified conditions were created by dampening paper towels placed at the bottom of the sink). Following incubation with primary antibodies, slides were rinsed three times with TRIS-HCl saline buffer. Secondary link reagent (see table 5) corresponding to the isotype of the primary antibody was then applied to tissue samples for 30 minutes. Slides were then rinsed three times with TRIS-HCl saline buffer. Substrate chromogen (DAB+ see table 6) was applied to tissue samples as the visualisation system for 10 minutes. Test sections were once again washed with TRIS-HCl saline buffer and subsequently washed with deionised water.

Test slides were then removed from the autostainer and rinsed in running water, then counterstained with Mayers haematoxylin for 5 minutes to elaborate nuclei as per H & E staining procedure as previously described. Tissue sections were checked under microscope to ensure nuclei were sufficiently stained. Tissue sections were then dehydrated, cleared and mounted in Dako mounting media (table 2). Test slides were then dried over a hot plate at 60°C overnight in order to dry mounting medium. Date of run was recorded on each completed test slide at the end of a run.

Figure 2.8: Dako Coverslipper

2.12 Controls

Tissue controls were selected from material known to possess the antigen of interest and used to validate each run of the immunostaining. The same control material was also used to validate the staining of tissue as a result of using the two different heat retrieval methods (autoclave vs PT link device) that came about as result of the purchase of new equipment (PT link device).

Isotype negative controls were utilised as reagent controls i.e. for each biopsy a serial section of that slide had isotype matched primary antibody applied to replace the pSmad2/3 primary. All the negative controls that were conducted were found to be stained negative indicating that the immunochemistry method did not label non-specific antigens associated with either the F_c region of the primary antibodies or the secondary link reagents. Reagents used in this study were controlled by utilising standard diluents and appropriate reagents as well as documenting each immunostaining run that was conducted to ensure quality control.

Humidity in the autostainer was maintained by laying paper towels immersed in deionised water and room temperature was based on building-wide temperature of 22℃.

2.13 Histological and immunohistochemical analysis

Computer-assisted image analysis was conducted using Leica DM2500 microscope (Leica Microsystems, Germany) and Leica camera (Supplier- Leica Bioscience, Product code- DFC495) (Figure 2.9) that was linked to an image analysis software, Image Pro Plus Version 7.0 (Media Cybernetics, US).

Figure 2.9: Biopsy image analysis equipment with Leica DM2500 microscope and digital camera

On each slide, two biopsy sections were fixed for analysis as shown by drawing circles around them in Figure 2.10. First, as many pictures as possible were taken from both of the tissue sections from the area of interest (for this study it was mainly epithelium, Rbm, and lamina propria) for each slide. Only subjects with sufficient amounts of tissue were analysed. Sections were photographed if they had intact epithelium and LP, with no holes or tissue damage. Most subjects had one section suitable for imaging; where two or more sections from a single subject were suitable, all images were grouped together and treated as if from the same section. Once photographed, five images were randomly chosen from each subjects' 'pool' of images and used for measurements. The number of epithelial cells, cells in the Rbm, blood vessels in the Rbm and LP were stained by pSmad2/3 was counted using the automated software (Image Pro Plus) (Figure 2.9). Cells and vessels were classified by the investigator, based on their morphology.

Figure 2.10: Showing two biopsy sections fixed on a pSmad slide with black circles around them, arrows indicate the location of the biopsies.

The positively stained blood vessels up to 150µ deep into lamina propria (Figure 2.11) were measured. These numbers were presented as cells and vessels per unit length of Rbm and per unit area of LP. The percentage of vessels in the Rbm and LP stained for pSmad2/3 was calculated by dividing the number of vessels stained for pSmad2/3 by the total number of vessels. All slides were coded and randomised by an independent person and then counted in a single batch by this investigator who was blinded to subject and diagnosis. For quality assurance and validity purposes, randomly selected slides were measured and matched with results from this investigator by another researcher who is very experienced at image analysis.

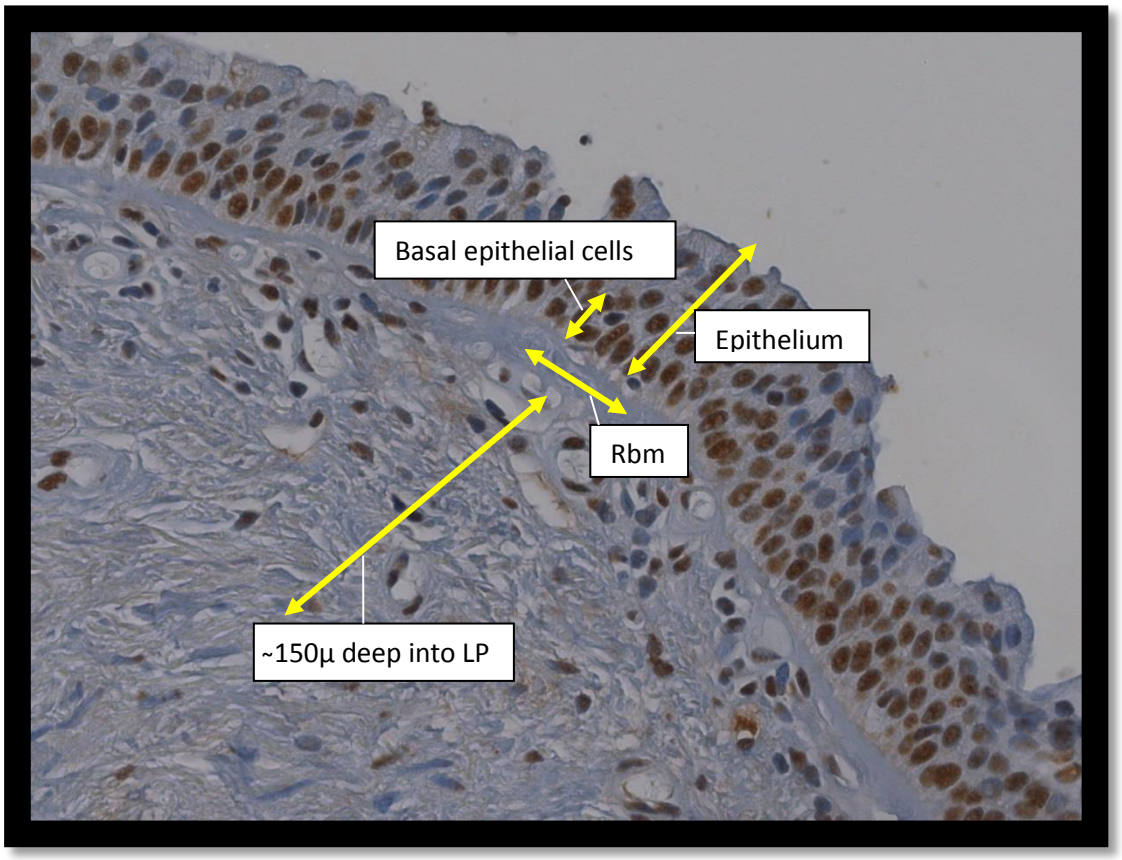

Figure 2.11: Showing a biopsy image under the microscope for analysis (Magnifications X40)

Chapter 3 - Results

Transforming growth factor beta (TGFβ) is one of the most important tissue and cell regulators (52, 82, 92, 132). Studies on lungs have shown that TGFβ can induce pathological changes through Smad protein activation (68, 81, 87, 135). TGFβ activity is shown to be increased among smokers, particularly with chronic obstructive pulmonary disease (COPD) group (118). A cross-sectional study was designed to investigate the phosphorylated Smad2/3 (pSmad2/3) pathway between smokers, smokers with COPD, ex-smokers with COPD and non-smokers with healthy lungs.

A longitudinal study was also designed, using the same cohort as the cross-sectional study, to study the effects of inhaled corticosteroids (ICS) on COPD airways. ICS has been widely used for the treatment of COPD for the last two decades (136). A study on bronchial vascular remodelling in COPD patients treated with steroids showed significant reduction in positive TGFβ expression compared to non-treated COPD group (137). This longitudinal study was designed to investigate the positive immunostaining of pSmad2/3 on vascular remodelling for the COPD group who were on ICS and compared with the placebo group.

3.1 Subjects demographics

For the cross-sectional study, 57 people were recruited, 15 were healthy non-smokers (NC), 13 were smokers with normal lung function (NLFS), 15 were current-smokers with COPD (COPD-CS), and 14 were ex-smokers with COPD (COPD-ES). Due to insufficient tissues from the samples from 3 of the control subjects, 12 participants' tissues were used for study. 12 of COPD ex-smokers subjects' samples were used for analysis as the other 2 did not have sufficient tissues on their samples.

For the longitudinal study, 12 COPD subjects from the same cohort had sufficient tissue to perform the analysis of the effects of ICS. Nine of these subjects were treated with fluticasone propionate (0.5mg) twice daily for six months and three received a placebo.

The subjects' demographics can be seen in table 3.1 and 3.2. There were no statistically significant differences in the male to female ratios across the groups ($p>0.05$). People with COPD smoked significantly more than normal lung function smokers ($p<0.05$); however, given the difference in age between the groups ($p<0.05$) this is not unexpected as COPD groups were older and they had more time to smoke. People with COPD had significantly lower lung function than non-smokers and smokers with normal lung function ($p<0.05$). Subjects that are used for the longitudinal study did not have any statistical significant difference for lung function ($p>0.05$), smoking pack-years ($p>0.05$), nor the age ($p>0.05$) (table 3.2).

Table 3.1: Demographics for cross-sectional study

Groups	Normal Controls (n=15)	Smokers (n=13)	COPD Smokers (n=15)	COPD Ex-smokers (n=14)	p value
Age (years)	54 (20-68)	46 (30-66)	60 (48-69)	62 (53-69)	<0.05
Male/Female	7/8	9/4	9/6	9/5	>0.05
Smoking history (Pack-years)	0	32 (10-57)	44 (18-82)	66 (18-150)	0.02* 0.01^{+}
FEV1% predicted (Post-BD)	119 (114-124)	99 (78-125)	79 (55-100)	80 (55-105)	<0.05
FEV1/FVC% (Post-BD)	82 (71-88)	77 (70-96)	59 (47-68)	57 (38-68)	<0.05

Demographics of the study population.
Post-BD= Post- bronchodilator response after 400µg of salbutamol. FEV1= forced expiratory volume in 1 second, FVC= forced vital capacity. Smoking history in pack-years was calculated by multiplying the number of packs of cigarettes smoked per day by the number of years the person has smoked.
Data expressed as median (range).
*COPD current-smokers vs normal lung function smokers.
$^{+}$COPD ex-smokers vs normal lung function smokers.

Table 3.2: Demographics for longitudinal study

Groups	Placebo (n=3)	Steroid (n=9)	p value
Age (years)	61 (56-66)	60 (48-69)	0.73
Male/Female	2/1	6/3	1.00
Smoking history (Pack-years)	59 (51-71)	46 (18-82)	0.23
FEV1% predicted (Post-BD)	68 (55-76)	75 (55-105)	0.28
FEV1/FVC% (Post-BD)	59 (38-63)	56 (47-65)	0.86

Demographics of the study population.
Post-BD= Post- bronchodilator response after 400µg of salbutamol. FEV1= forced expiratory volume in 1 second, FVC= forced vital capacity. Smoking history in pack-years was calculated by multiplying the number of packs of cigarettes smoked per day by the number of years the person has smoked.
Data expressed as median (range).

3.2 Cross-sectional study

General morphology

In COPD structural changes are observed in airways, such as goblet cell hyperplasia, mucus hypersecretion (67, 138), infiltration of numerous cells, and remodelling of the extracellular matrix (39, 139).These changes worsen as the disease progresses and are not reversed by smoking cessation (54).

Normal non-smokers had pseudostratified epithelial layer, with all epithelial cells adhered to each other in one layer and the epithelium was not fragmented. This is demonstrated in figure 3.1A. The epithelium, shown by the blue line in 3.1A, covered the most superficial part of mucosa and the yellow line shows what were considered basal epithelial cells in this study. The epithelial layer was attached to the reticular basement membrane (Rbm) (the orange line), which was a smooth, unbroken structure in normal non-smokers. The Rbm lies beneath the epithelium and separates it from the lamina propria (LP). The LP, shown by green line in 3.1A was made up of loose connective tissue and contained cells and blood vessels. Smokers with normal lung function had similar structure, however, there were occasionally gaps between epithelial cells (shown by arrows), and the overall structure began inclining towards stratified morphology, as seen in 3.1B. COPD current-smokers had more fragmented epithelium, losing their cuboidal morphology and at some points becoming almost detached from the basement membrane, shown by arrows in figure 3.1C. Across all the groups, there were large ranges of thickness of epithelium. An example of this can be seen in figure 3.2 for the COPD current-smokers group. COPD current-smokers particularly appeared to segregate into two sub-groups, one with epithelial hyperplasia (3.2A) and one that demonstrated normal epithelial thickness (3.2B), this was statistically significant ($p<0.01$). COPD ex-smokers also had epithelium which had lost their cuboidal morphology and appear more ragged and disorganised, as shown by arrows in 3.1D.

The reticular basement membranes (Rbm) in normal non-smokers were narrow, smooth and consistent, underlining the epithelium distinctly as shown by orange line in 3.1A. Smokers with normal lung function had similar Rbm structure lining the epithelium (arrowheads in 3.1B). For COPD current-smokers, the Rbm seemed thicker and fragmented, shown by arrowheads, with cells present in the clefts, as shown by the red circles in 3.1C. COPD ex-smokers also seemed to have thickened and fragmented Rbms, indicated by arrowheads, and exhibit cellularity (red circle in 3.1D). COPD current-smokers also had blood vessels in the Rbm as shown in figure 3.3B by green arrows.

The structure of the lamina propria (LP) appeared to be similar across all the groups (figure 3.1), however, COPD current-smokers seemed to have more blood vessels than non-smokers, which can be in seen in figure 3.3, where the LP vessels are indicated by red circles, and also shown later on figure 3.8, however, this was not quantitatively measured.

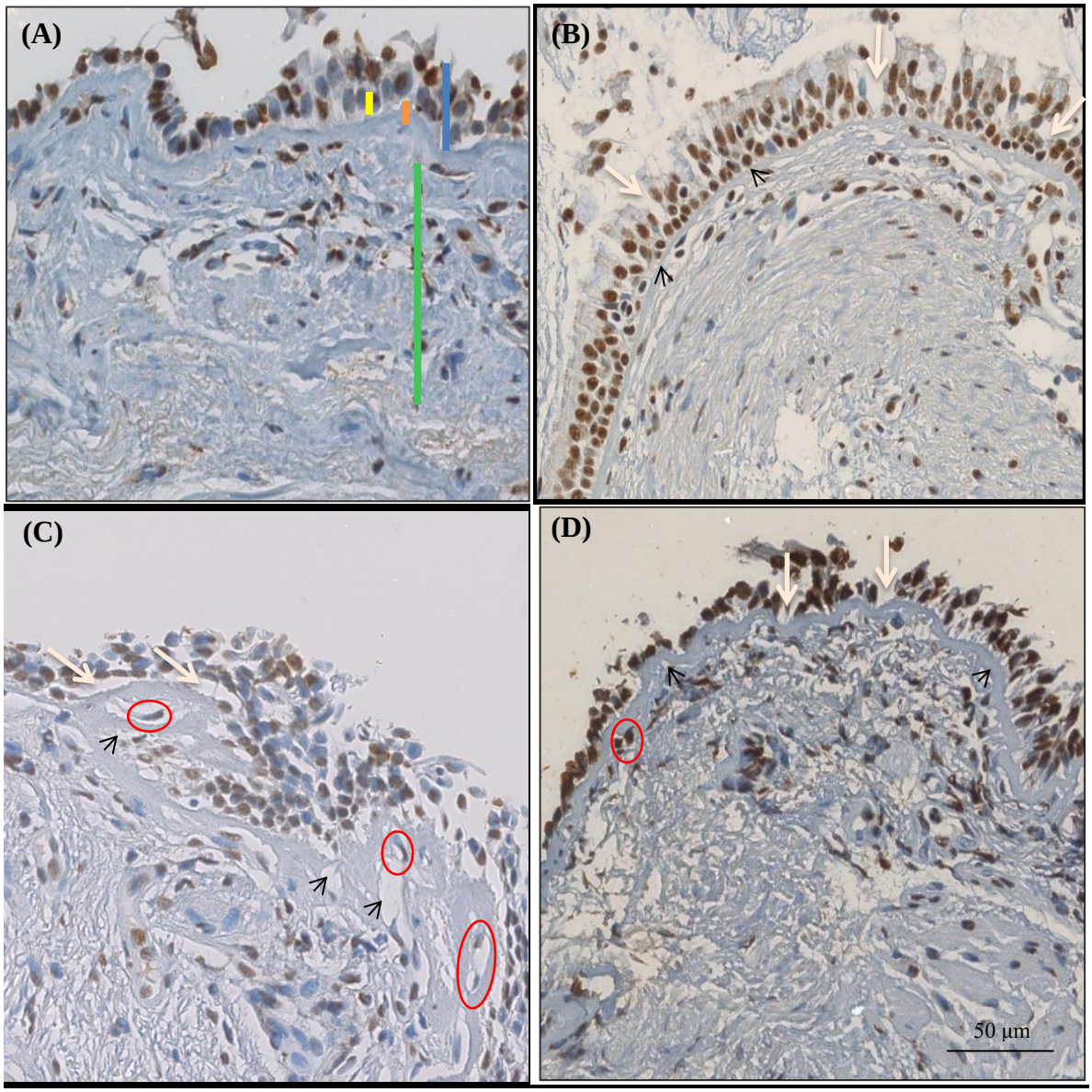

Figure 3.1 Microphotograph from subjects from each group in the study showing biopsies stained with haematoxylin and an antibody directed against phosphorylated Smad2/3 (pSmad2/3).

Biopsies from patients from each group, panel A shows normal non-smokers (NC), panel B shows smokers with normal lung function (NLFS), panel C shows COPD current-smokers and panel D shows COPD ex-smokers. Each picture is a general representation of the entire group, showing pSmad2/3 staining of the epithelium and sub-epithelial layers. On panel A, the blue line indicates the epithelium area, the yellow line shows the basal epithelial cells, which were measured 15µm from the basement membrane towards the epithelium, the orange line indicates the reticular basement membrane (Rbm) below the epithelium, and the green line indicates the lamina propria (LP) underneath the basement membrane, where the blood vessels were measured to a depth of 150µm from the internal (deep) border of the Rbm. In panel B, the white arrows show the gaps between epithelial cells and the black arrowheads show the Rbm lining the epithelium. In panel C, the white arrows show how epithelial cells losing their attachment to the basement membrane in COPD current-smoker subject and the black arrowheads and red circles show clefts and cells in the clefts

respectively. In panel D, the white arrows show the distorted epithelium and red circle shows cells in the Rbm. Original magnification X 40. Scale = 50µm.

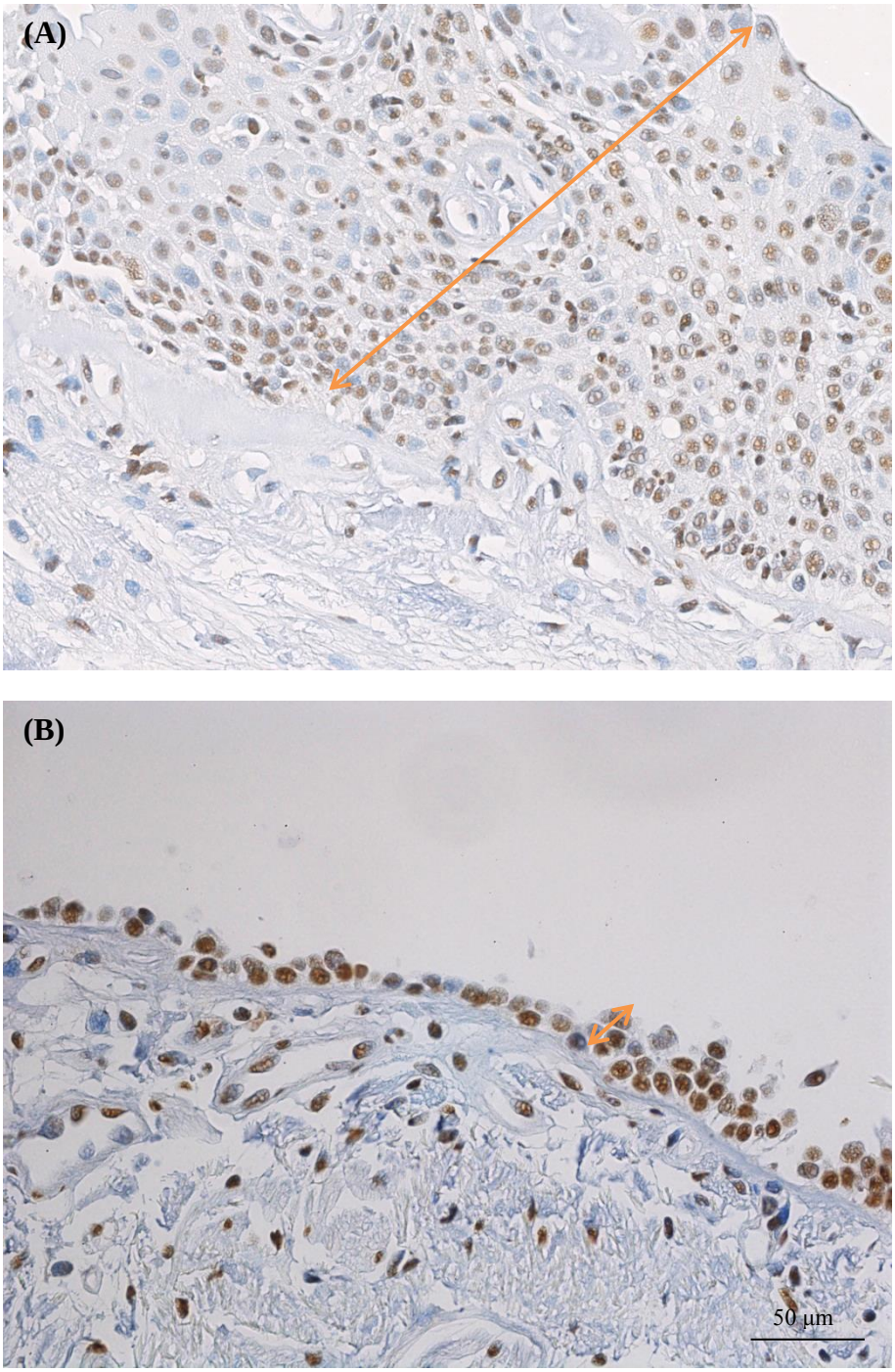

Figure 3.2: Variability in epithelium thickness in COPD current-smokers group.
The upper panel (A) shows thickened and disorganised epithelium as shown by orange arrows, whereas the lower panel (B) shows thin epithelium as indicated by orange arrow. Original magnification X 40. Scale = 50µm.

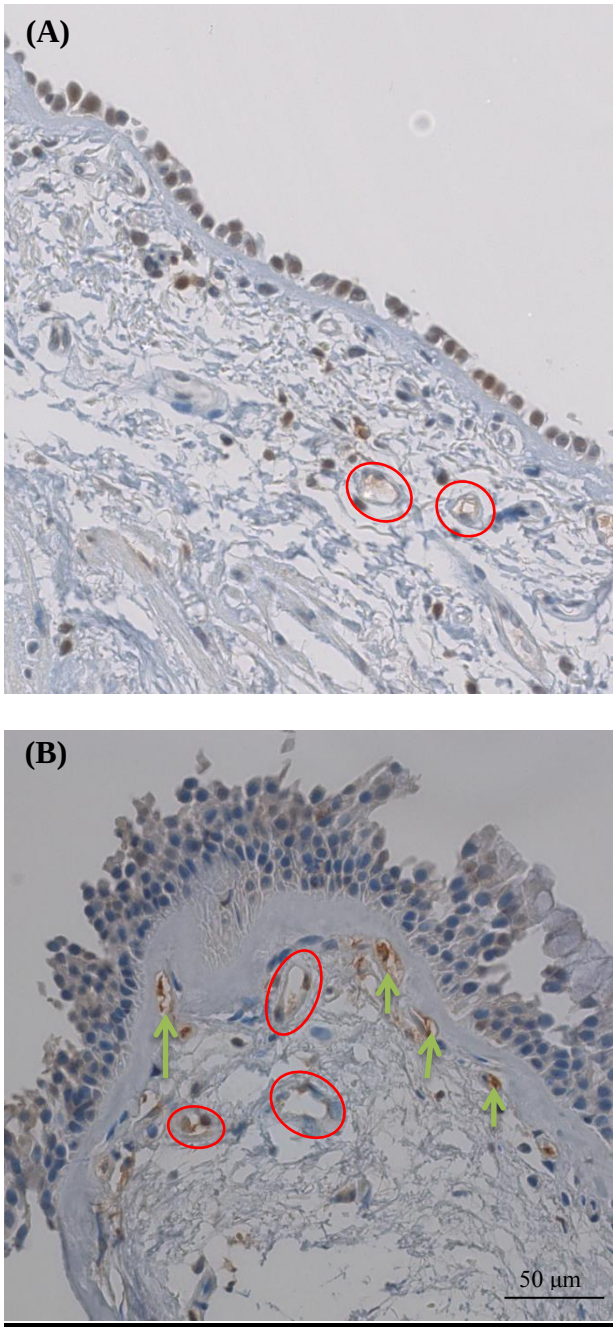

Figure 3.3: Variability in blood vessels in the COPD current-smokers.
The upper panel (A) shows normal non-smokers, with few blood vessels in the LP as shown by red circles, whereas the lower panel (B) shows a number of blood vessels positively immunostained for pSmad2/3in the Rbm and LP of COPD current-smokers as shown by green arrows and red circles respectively. Original magnification X 40. Scale = 50µm.

In order to determine the phosphorylation of Smad2/3 in these morphological changes, different areas of the tissues for 4 different groups were analysed.

3.3 Epithelial cells

In COPD, the epithelium undergoes numerous changes including hyperplasia and goblet cell hypersecretion (139, 140). Transforming growth factor beta (TGFβ), being a multifunctional cytokine, induces structural, cellular, and inflammatory changes in the lungs (92, 141). Smad is the predominant pathway through which TGFβ regulates its function, using phosphorylated (activated) Smads (pSmads) (132, 133). Hence, the aim was to investigate whether pSmad2/3, the most commonly seen pSmads complex (83, 88, 142), is active in the epithelium of the COPD.

In order to study the pSmad2/3 immunostaining, the epithelial cells stained positive for pSmad2/3 for the four groups were counted. There were no statistically significant differences for pSmad2/3 staining in the epithelium across the four groups ($p>0.05$), and none of the groups were significantly different from controls ($p>0.05$) as shown in Figure 3.4A.

However, there were statistically significant differences among the four groups for percentage epithelium ($p=0.01$), as shown in figure 3.4B. COPD current-smokers had higher percentage of epithelial cells stained for pSmad2/3 than controls ($p=0.04$). COPD ex-smoker also had higher percentage of epithelial cells than controls ($p=0.01$). Normal lung function smokers had the same percentage of positive pSmad2/3 epithelial cells as controls ($p>0.05$) (figure 3.4B).

Table 3.3: The number of epithelial cells in total and positively stained for pSmad2/3 (raw data in appendix 1)

	Normal Controls (n=12)	**Smokers (n=13)**	**COPD Smokers (n=15)**	**COPD Ex-smokers (n=12)**	**p value**
pSmad2/3 cells	0.19/μm (±0.08)	0.20/μm (±0.11)	0.19/μm (±0.10)	0.21/μm (±0.07)	$>0.05^{+}$ $>0.05^{++}$
Total cells	0.21/μm (±0.09)	0.22/μm (±0.11)	0.19/μm (±0.10)	0.22/μm (±0.08)	$>0.05^{+}$ $>0.05^{++}$

$^{+}$ represents p value across all 4 groups, $^{++}$ represents p value for all 3 groups against control. The data are presented as mean (standard deviation). The mean data are represented per unit of the reticular basement membrane.

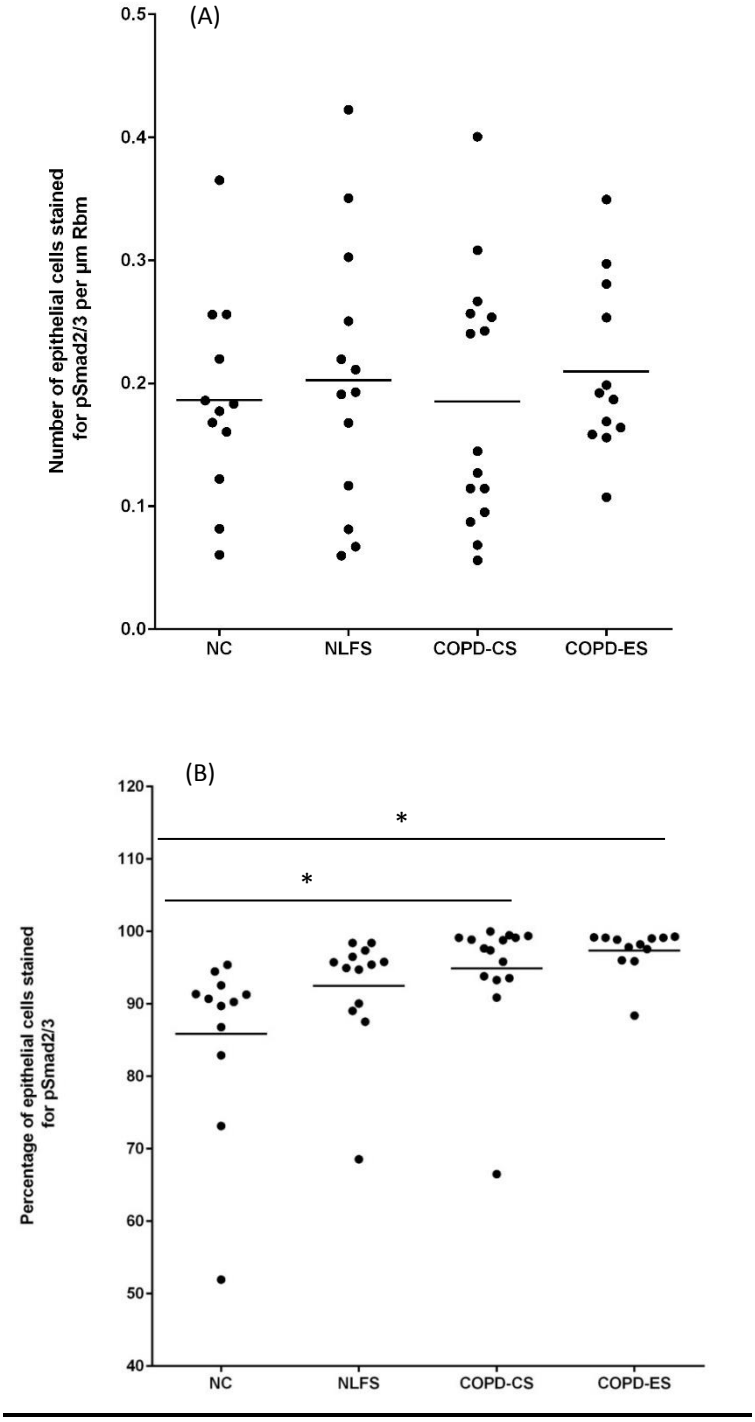

Figure 3.4: (A) Epithelial cells per µm of Rbm stained for pSmad2/3; the epithelial cells were compared in healthy non-smokers (NC), normal lung function smokers (NLFS), current-smokers with COPD (COPD-CS), and ex-smokers with COPD (COPD-ES). (B) The percentages of epithelial cells stained for pSmad2/3; the percentages were compared in healthy non-smokers (NC), normal lung function smokers (NLFS), current-smokers with COPD (COPD-CS), and ex-smokers with COPD (COPD-ES). The lines indicate the mean values for each group. (* indicates a p value <0.05, ** indicates a p value <0.01 and *** indicates a p value <0.001). For each subject, 5 images were obtained and the numbers of positively stained cells in the epithelium were counted for each picture. Then, the numbers of positive cells per unit for the same subject were calculated by dividing the total number of cells by the total length of the basement membrane. Each point on the graph shows the data for a single subject.

3.4 Basal epithelial cells

The proportion of epithelial cells showed a significant increase for the COPD groups and it is possible that the airway basal cells are more active than the apical cells as airway basal cells are central to the pathogenesis of smoking-associated lung diseases (143). This study investigated the pSmad2/3 staining in the basal epithelial cells between the 4 groups, so as to study the migratory characteristics of the basal epithelial cells. These cells are thought to undergo epithelial to mesenchymal transition (EMT) and migrate through the basement membrane, as they are closest to the membrane and also the site of the earliest abnormalities in smokers' lungs (143). Since no basal cell markers were used to distinguish them from the other non-stem cells, in this study the basal epithelial cells are defined as any epithelial cells within 15μm of the basement membrane.

In order to determine the pSmad2/3 staining for the basal epithelium, the basal epithelial cells stained positive were counted for the subjects. There were no statistically significant differences for pSmad2/3 staining in the basal epithelial cells across the four groups ($p>0.05$), and none of the groups were significantly different from controls ($p>0.05$) as shown in Figure 3.5.

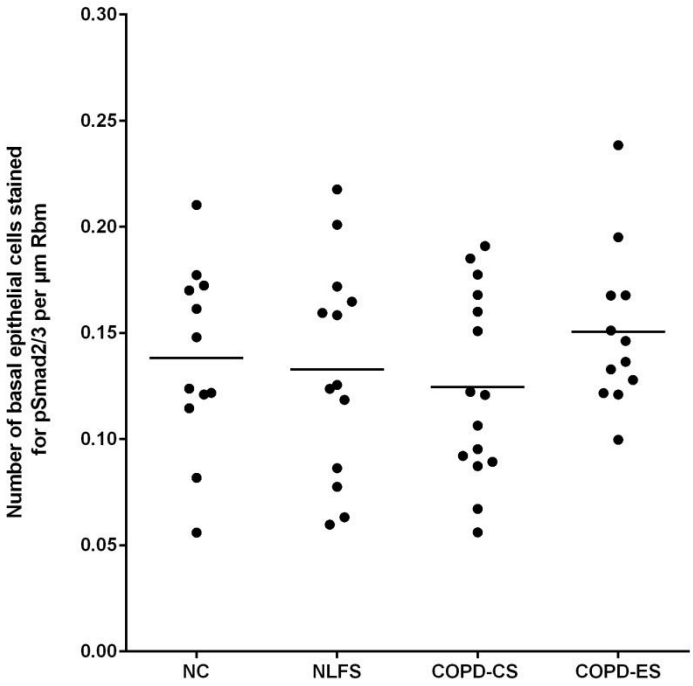

Figure 3.5: Basal epithelial cells per μm of Rbm stained for pSmad2/3; the basal epithelial cells were compared in healthy non-smokers (NC), normal lung function smokers (NLFS), current-smokers with COPD (COPD-CS), and ex-smokers with COPD (COPD-ES). The lines indicate the mean values for each group. (* indicates a p value <0.05, ** indicates a p value <0.01 and *** indicates a p value <0.001). For each subject, 5 images were obtained and the numbers of positively stained basal epithelial cells (15μm from the basement membrane towards the epithelium) were counted for each picture. Then, the numbers of positive cells per unit for the same subject were calculated by dividing the total number of cells by the total length of the basement membrane. Each point on the graph shows the data for a single subject.

3.5 Rbm cells

COPD airways have been shown to have cells present in the reticular basement membrane (Rbm) (29). These cells have been shown to be positive for EMT biomarkers that are broadly referenced in EMT studies, matrix metalloproteinase-9 (MMP-9), the fibroblast protein (S100A4) and mesenchymal marker, vimentin (29, 67, 144). To rule out the possibility of these cells being inflammatory cells, the biopsies were stained for neutrophil marker, macrophage (CD68) marker, and very few neutrophils and macrophages were found in the Rbm (29). Therefore, the question arises whether pSmad2/3 are up-regulated in the Rbm cells to drive TGFβ pathway in the COPD groups. This study investigated the Rbm cells showed positive pSmad2/3 staining for the 4 different groups.

In order to measure the pSmad2/3 staining for the Rbm cells, the numbers of positive pSmad2/3 cells in the Rbm were counted. There were statistically significant differences for pSmad2/3 staining in the Rbm cells across the four groups (p=0.01). COPD ex-smokers group was significantly different from controls (p=0.01) for pSmad2/3 staining in the Rbm cells, as shown in Figure 3.6. Neither COPD current-smokers nor normal lung function smokers were significantly different from controls (p>0.05).

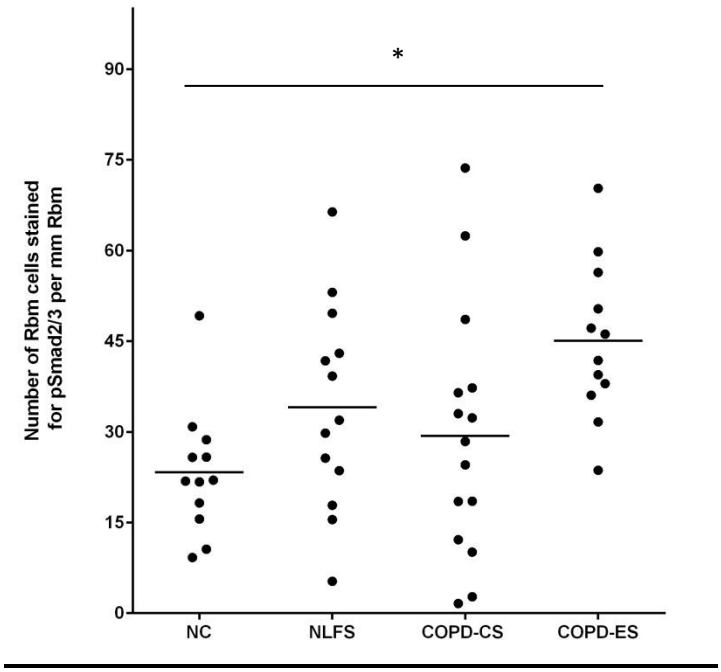

Figure 3.6: Rbm cells per mm of Rbm stained for pSmad2/3; the Rbm cells are compared in healthy non-smokers (NC), normal lung function smokers (NLFS), current-smokers with COPD (COPD-CS), and ex-smokers with COPD (COPD-ES). The lines indicate the mean values for each group (* indicates a p value <0.05, ** indicates a p value <0.01 and *** indicates a p value <0.001) For each subject, 5 images were obtained and the numbers of positively stained Rbm cells were counted for each picture. Then, the numbers of positive cells per unit for the same subject were calculated by dividing the total number of cells by the total length of the basement membrane. Each point on the graph shows the data for a single subject.

3.6 Rbm vessels

Angiogenesis is one of the hallmarks of type 3 EMT which is associated with cancer progression and other malignancies (60). Hypervascularity was evident in the Rbm during airway remodelling in smokers with COPD, and TGFβ immunostaining was increased in these blood vessels (118). This study investigated the blood vessels in the Rbm to quantify the pSmad2/3 staining in the 4 groups in order to study which pathway TGFβ is acting through.

In order to investigate the pSmad2/3 positive blood vessels, the positive blood vessels were counted in the basement membrane and compared between the groups. There were statistically significant differences for pSmad2/3 staining in the Rbm blood vessels across the four groups ($p=0.001$). COPD current-smokers group was significantly different from controls ($p=0.01$) for pSmad2/3 staining in the Rbm vessels, as shown in figure 3.7A. Furthermore, COPD current-smokers group was also significantly different from normal lung function smokers ($p=0.001$) and from COPD ex-smokers ($p=0.03$), as shown in figure 3.7A. Neither normal lung function smokers nor COPD ex-smokers were significantly different from controls ($p>0.05$).

There were statistically significant differences among the four groups for percentage pSmad2/3 staining of Rbm vessels ($p<0.01$), as shown in figure 3.7B. COPD current-smokers had higher percentage of Rbm vessels stained for pSmad2/3 than controls ($p=0.002$). Moreover, COPD current-smokers group was also significantly different from normal lung function smokers ($p<0.01$). Neither COPD ex-smokers nor normal lung function smokers were significantly different from controls ($p>0.05$) (figure 3.7B).

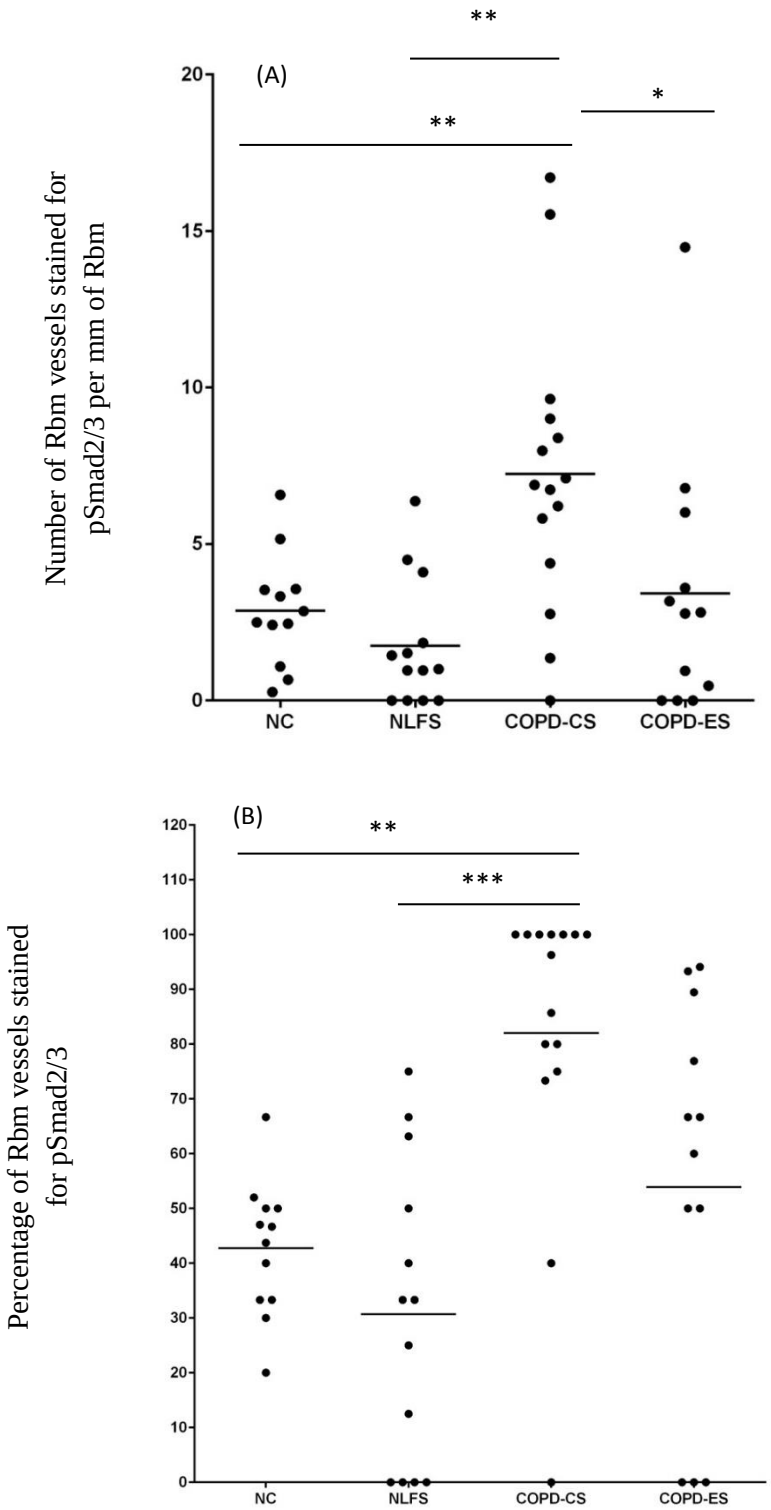

Figure 3.7: (A) Rbm vessels per mm of Rbm stained for pSmad2/3; (B) the percentage of Rbm vessels, the Rbm vessels are compared in healthy non-smokers (NC), normal lung function smokers (NLFS), current-smokers with COPD (COPD-CS), and ex-smokers with COPD (COPD-ES). The lines indicate the mean values for each group (* indicates a p value <0.05, ** indicates a p value <0.01 and *** indicates a p value <0.001). For each subject, 5 images were obtained and the numbers of positively stained Rbm vessels were counted for each picture. Then, the numbers of positive vessels per unit for the same subject were calculated by dividing the total number of vessels by the total length of the basement membrane. Each point on the graph shows the data for a single subject.

3.7 LP vessels

Bronchial vascular remodelling has also been shown to occur in lamina propria (LP) (65, 137). TGFβ immunostaining was increased in these blood vessels (118) and therefore this study investigated the blood vessels in the LP to quantify the pSmad2/3 staining in the 4 groups in order to study which pathway TGFβ is acting through in LP vessels.

In order to investigate the pSmad2/3 positive blood vessels in LP, the positive blood vessels 150μm deep into the LP were counted and compared between the groups. There were statistically significant differences for pSmad2/3 staining in the LP blood vessels across the four groups ($p=0.01$). COPD current-smokers group was significantly different from controls ($p=0.01$) for pSmad2/3 staining in the LP vessels, as shown in figure 3.8A. Moreover, COPD current-smokers group was also significantly different from normal lung function smokers ($p=0.04$) and from COPD ex-smokers ($p=0.03$), as shown in figure 3.8A. Neither normal lung function smokers nor COPD ex-smokers were significantly different from controls ($p>0.05$).

There were statistically significant differences among the four groups for percentage pSmad2/3 staining of LP vessels ($p<0.01$), as shown in figure 3.8B. COPD current-smokers had higher percentage of LP vessels stained for pSmad2/3 than controls ($p<0.01$). COPD ex-smokers also had higher percentage of LP vessels stained for pSmad2/3 than controls ($p=0.01$). Normal lung function smokers had the same percentage of pSmad2/3 staining of LP vessels as controls ($p>0.05$) (figure 3.8B).

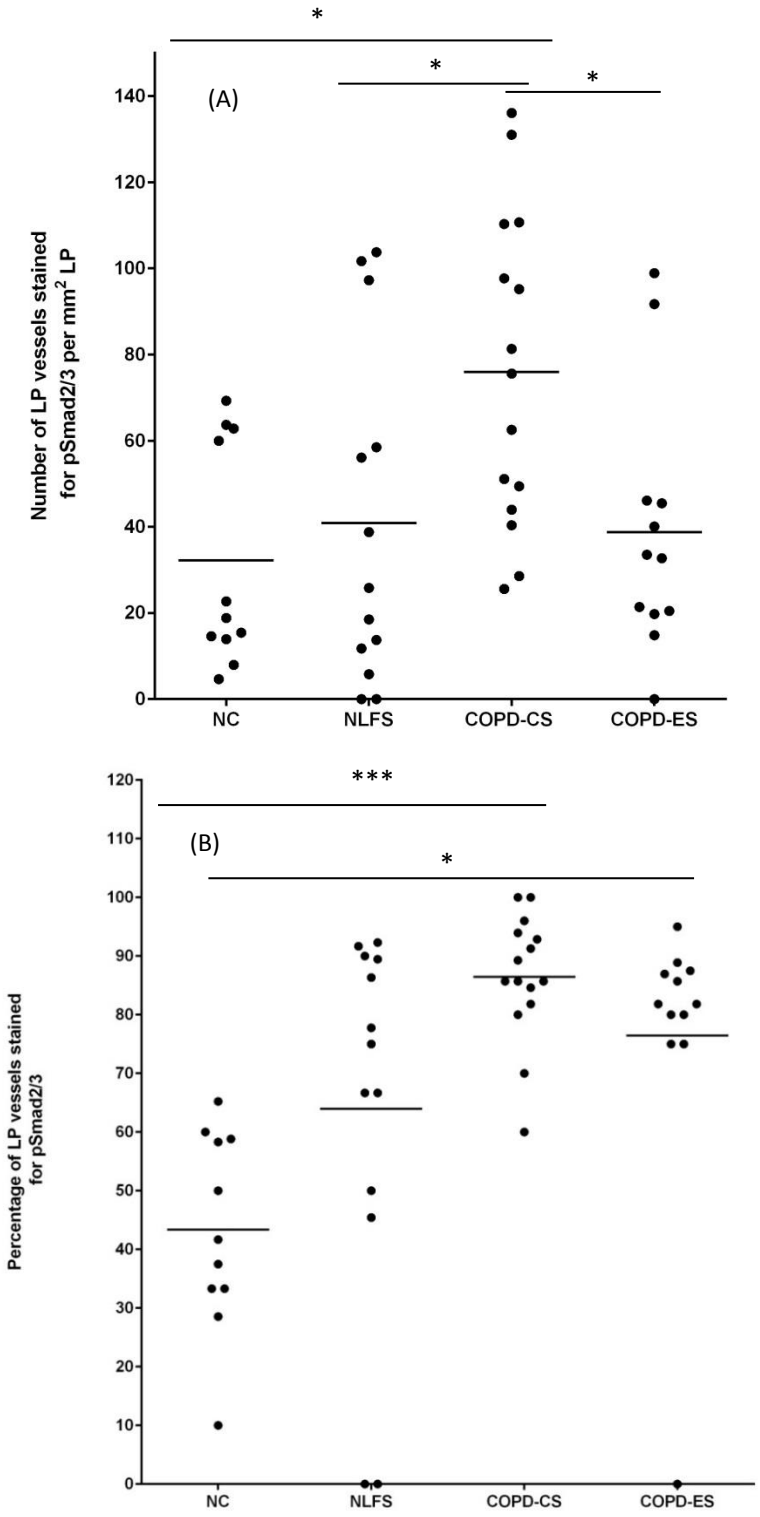

Figure 3.8: (A) LP vessels per mm² stained for pSmad2/3; (B) the percentage of LP vessels, the LP vessels are compared in healthy non-smokers (NC), normal lung function smokers (NLFS), current-smokers with COPD (COPD-CS), and ex-smokers with COPD (COPD-ES). The lines indicate the mean values for each group (* indicates a p value <0.05, ** indicates a p value <0.01 and *** indicates a p value <0.001). For each subject, 5 images were obtained and the numbers of positively stained LP vessels were counted for each picture. Then, the numbers of positive LP vessels (150µ deep into lamina propria) per unit for the same subject were calculated by dividing the total number of vessels by the total area of the lamina propria. Each point on the graph shows the data for a single subject.

3.8 Inhaled corticosteroid effects on vascular remodelling in COPD airways: A longitudinal study

The use of inhaled corticosteroids (ICS) has been shown to be beneficial in COPD, including reducing the rate of exacerbations in COPD, reducing the rate of decline in lung function, and improving the quality of life (145, 146). The increased angiogenic activity in the Rbm and LP has been reported to respond to treatment with ICS (147, 148). Therefore, this study investigated the effects of ICS on pSmad2/3 staining for the COPD blood vessels in order to study whether the ICS is working through pSmad2/3 proteins.

To assess the ICS effects on pSmad2/3 staining in the blood vessels, the number of vessels stained positive for pSmad2/3 in the Rbm and LP were counted from the COPD cohorts before and after 6 months of ICS treatment (0.5mg fluticasone propionate twice daily) and compared to the placebo group. There were no statistically significant differences in pSmad2/3 staining, neither in Rbm nor LP vessels for the treatment arm as compared to the placebo arm ($p>0.05$) (figure 3.9).

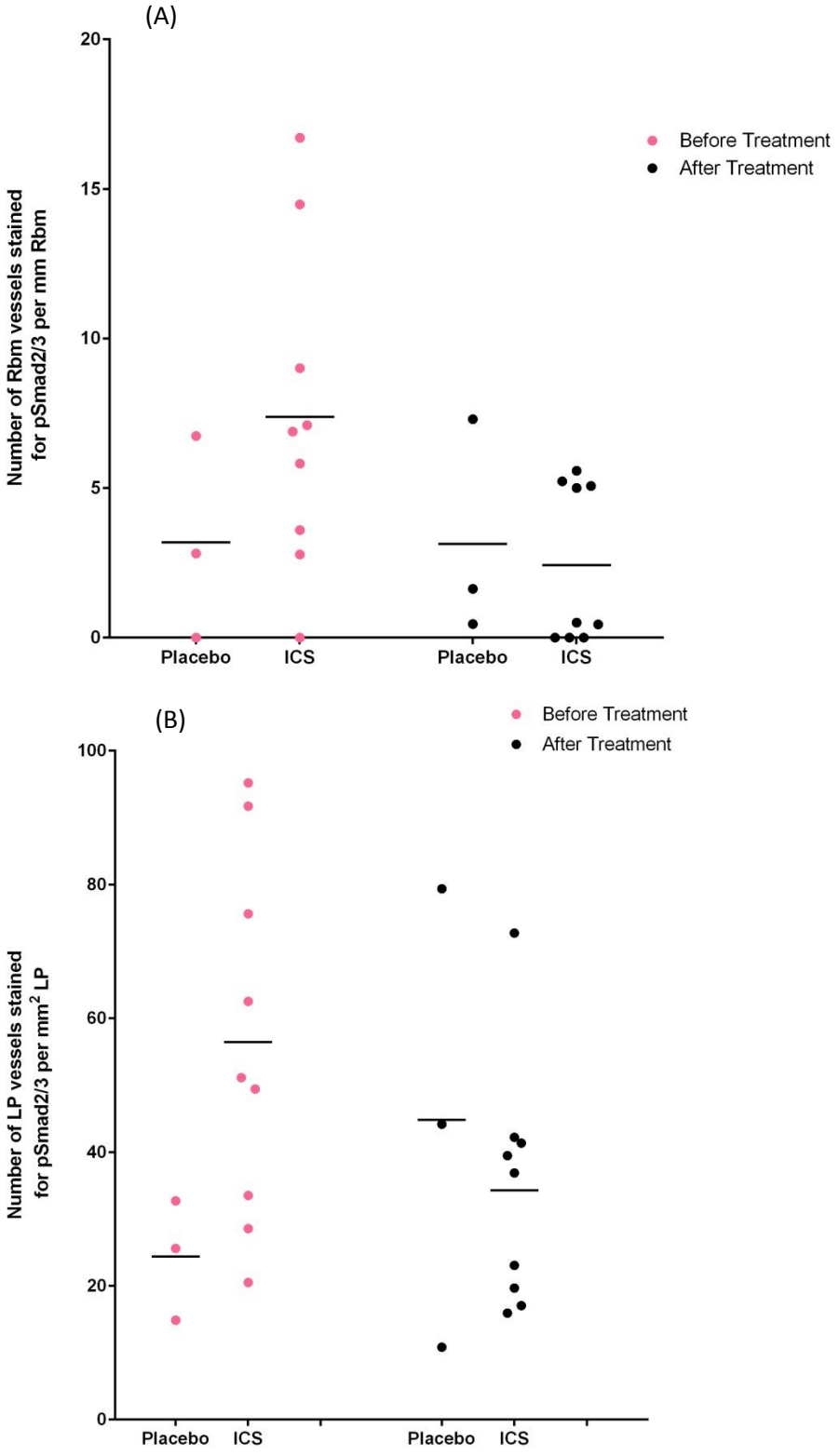

Figure 3.9: (A) Rbm vessels per mm stained for pSmad2/3; (B) LP vessels per mm^2 stained for pSmad2/3, compared between the placebo and treatment groups. The lines indicate the mean values for each group. For each subject, 5 images were obtained and the numbers of positively stained vessels were counted for each picture. Then, the numbers of positive vessels per unit for the same subject were calculated by dividing the total number of vessels by the total length of Rbm for Rbm vessels and total area of the LP for LP vessels. Each point on the graph shows the data for a single subject.

Chapter 4 - Discussion

4.1 General overview

This study has revealed novel aspects of airway remodelling in the airways in COPD patients with or without smoking effects. The main results can be summarised as follows:

1) The epithelium in patients with COPD had more phosphorylated Smad2/3 (pSmad2/3) immunostaining than healthy non-smokers, regardless of smoking status.
2) The basal epithelium in patients with COPD and smokers with healthy lungs were not different in pSmad2/3 immunostaining than non-smokers.
3) The reticular basement membrane (Rbm) appeared to be morphologically different in the COPD groups. It seemed thicker, fragmented and cells were present in the clefts. COPD ex-smokers had significantly more Rbm cells showing pSmad2/3 immunostaining than healthy non-smokers.
4) There were more pSmad2/3 immunostaining in the blood vessels in the Rbm for current-smokers with COPD than the non-smokers with healthy lungs. However, this was not observed for smokers with normal lung function or ex-smokers with COPD.
5) There were more pSmad2/3 immunostaining in the blood vessels in the lamina propria (LP) for COPD groups than in non-smokers with healthy lungs, but not in smokers with normal lung function.
6) Inhaled corticosteroids had no effects on pSmad2/3 immunostaining on blood vessels in COPD airways.

4.2 Epithelial layer

The current study showed increased pSmad2/3 immunostaining in the epithelial cells of COPD patients, both for current and ex-smokers compared to healthy subjects who were non-smokers *in vivo*. However, the basal epithelium did not show any significant difference for pSmad2/3 immunostaining for the COPD and smokers groups.

In the airways of smokers and patients with COPD, epithelial-mesenchymal transition (EMT) was shown in bronchial epithelial cells and it was also found that cigarette smoke extract promoted the phosphorylation of Smad3 in the bronchial epithelial cells (67). However, their study was focused on molecular methods and *in vitro* models. They measured phosphorylated Smad3 by protein array technology (67). Moreover, another *in vitro* study demonstrated that Smad2/3 signaling pathways that were activated by TGFβ caused EMT-related changes in pulmonary epithelial cells (142). Based on my findings and these findings, it may suggest that more Smad2/3 proteins are phosphorylated in the COPD airways and cigarette smoking may play a role in this, maybe by activating the TGFβ pathway, activating its downstream signaling Smad2/3 cascade through phosphorylation to promote COPD airway epithelium changes. This may contribute to the disease and possibly activate the transition of epithelial cells to cause them to lose their cuboidal morphology and become more mesenchymal.

However, there were limitations in this study that need to be considered. EMT markers that are broadly referenced in EMT studies such as the cytoskeletal proteins α-smooth muscle actin (α-SMA), vimentin (mesenchymal markers) (81) and epithelial E-cadherin, cytokeratin

(epithelial markers) (60) were not analysed to quantitate EMT in these biopsies. Additionally, for the basal epithelial cells that were counted in this study, the basal cell markers including Pdpn, Hopx and AGER (149, 150) could have been analysed to investigate the phosphorylation of the Smad2/3 in the progenitor cell population of the epithelium.

Despite the fact that airway basal cells were not properly identified, the current study revealed overall an increased proportion of epithelial cells showing pSmad2/3 immunostaining in patients with COPD. The pSmad2/3 proteins are possibly involved in the pathology of this disease, particularly in those who are smokers. Cigarette smoke may cause phosphorylation of Smad2/3 and other transcription factors, which may activate transcription of genes that result in pathological changes in the epithelium, which may include EMT. However, the precise role of cigarette smoking and pSmad2/3 in COPD still requires further investigation. The current study measured the positive staining of activated or phosphorylated Smad2/3 proteins in the epithelial cells, regardless of these proteins' location. Future study can focus on the location of these proteins in the cells, as this can potentially reveal more about its activity, as the Smad proteins are known to accumulate in the nucleus in response to TGFβ in order to have an effect (133). When Smads are phosphorylated after their receptor is activated by TGFβ, their affinity for cytoplasmic anchors are reduced and affinity for nuclear factors are increased, resulting in nuclear accumulation (141).

Additionally, it is also important to study the non-phosphorylated Smads as well as other Smads that are also involved in this pathway (133) and their involvement in COPD airways. In particular, inhibitory Smads 6 & 7 would be good subjects for study. If there is an up-regulation of Smads 6 & 7 concurrent with activation of Smad 2 & 3, then the Smad 2 & 3 may not be able to activate target gene transcription (Figure 4.1).

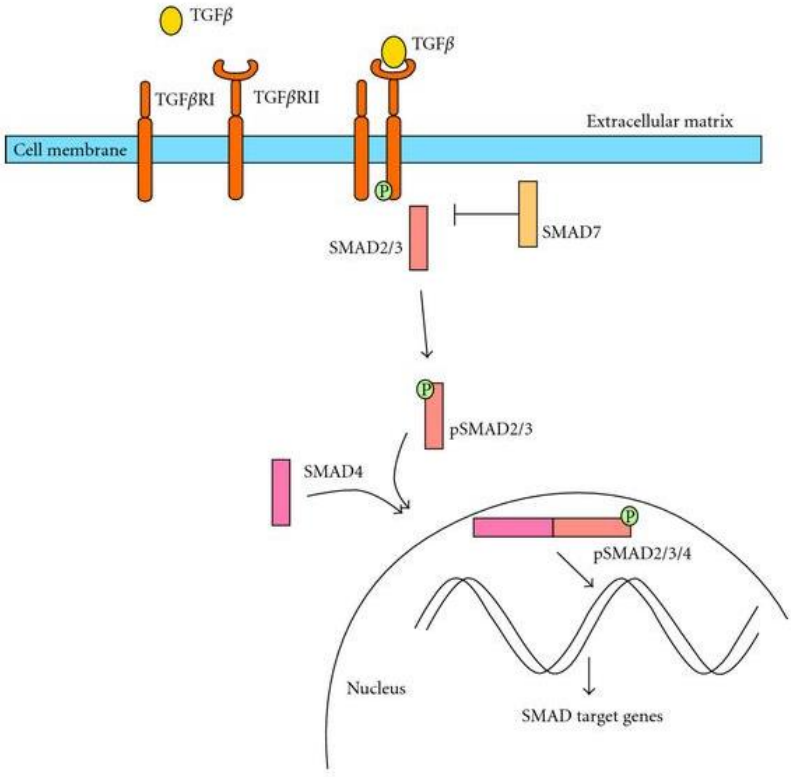

Figure 4.1: The TGFβ signaling pathway through Smads (125)

In this study, no differences were found in the total number of epithelial cells between the groups. The thickness of epithelium varied within the groups. Even non-smokers had a large range of epithelium thickness, even though the epithelium was compact, unlike the COPD and smokers groups. Epithelium is the first anatomical barrier that is exposed to the noxious particles of cigarette smoke and is involved in initiating the airway remodelling process through the release of inflammatory mediators (138), extracellular mediators including transforming growth factor beta (TGFβ) (84), and other fibrogenic mediators (151). Cigarette smoking is one of the key factors that lead to this airway remodelling manifested by metaplasia of the epithelium (152). The finding in this current study is contradictory to previous findings which show thickening of the epithelium (1, 43, 151). However, there can be a number of reasons for this. There just may be natural variation between subjects or it may be that non-smoking subjects were exposed to second hand smoke, as this study did not take that into consideration. COPD groups were significantly different for their smoking history from smokers with normal lung function. Therefore, the smokers with high and low pack years may contribute to the differences in the epithelial cells variation. Studies about pathological characteristics of the airways in COPD mention in addition to increased thickness of the wall (67, 153), epithelial goblet cell hyperplasia, squamous metaplasia and epithelial-mesenchymal transition (EMT) (41, 152).

Camara *et al* showed that upon stimulation of TGFβ, primary human bronchial epithelial cells undergo EMT through primarily Smad2/3 dependent mechanism (68). Milara *et al* also showed human bronchial epithelial cells undergo EMT after cigarette smoke extract exposure through the release of TGFβ and phosphorylation of Smad3 (67). In line with these results, this current study also shows that Smad2/3 is more phosphorylated in the epithelium of COPD than non-smokers, possibly driving the TGFβ pathway.. TGFβ has been considered to be a key factor in the induction of EMT in pulmonary epithelium (142), and Smad transcription factors are well known mediators of TGFβ signaling (133). Kolosova *et al* showed that within minutes of TGFβ1 exposure Smad2 and Smad3 were activated as was evidenced by their phosphorylation in pulmonary epithelial cells (142). They also showed that collagen I gene up-regulation were dependent on both Smads, Smad2 and Smad3 (142). The tissue deposition of type I collagen was caused by an increase in the rate of transcription, resulting in fibrotic EMT (154). The involvement of Smad3 in EMT causing fibrosis has been demonstrated *in vivo* and *in vitro* in other tissues such as the eye and kidney (155, 156), as well as the lungs (142). It is still not clear whether both Smad2 and Smad3 are responsible for TGFβ1 induced EMT. However, they may be involved in increased deposition of extracellular matrix (ECM) proteins in the sub-epithelial layer.

4.3 Sub-epithelial layer

The first sub-epithelial layer, the reticular basement membrane (Rbm) was morphologically different for the COPD groups from non-smokers and from smokers with healthy lungs. The Rbm seemed thicker, fragmented and cells were present in the clefts in patients with COPD. Liesker *et al* showed that Rbm thickening occurs in COPD (157). However, others have not found this difference (158, 159). Chanez *et al* showed that a subgroup of COPD with eosinophilic inflammation of airways had thicker Rbm than others (159), suggesting that Rbm thickening is an asthma phenotype (159). The discords about the Rbm thickness in COPD still remain to be elucidated. It can be proposed that the Rbm splitting could be the result of changes in ECM, new layers being formed by the epithelial cells, or may be degradation of the Rbm by proteolytic enzymes, due to stress or smoking. The major limitation in this current study should be highlighted that the thickness or the area of the Rbm was not measured or analysed and can be a potential area to be studied in future. Perhaps, the thickness of Rbm may be related to the cellularity that is seen in COPD patients.

Interestingly, this current study showed that the ex-smokers with COPD had a significant increase in pSmad2/3 immunostaining in the Rbm cells from non-smokers, as to however current-smokers with COPD were not significantly different from non-smokers. Previous works have shown that Rbm cells stain positive for the proteolytic enzyme, matrix metalloproteinase-9 (MMP-9), the early fibroblast transition marker, S100A4, vimentin, and other established EMT markers (29). A comparative analysis demonstrated that there were only very few neutrophils and macrophages, and concluded the majority of the cells in the Rbm were not inflammatory cells (29). These findings may indicate active migration of cells from the epithelium through the Rbm, and they may possess proteolytic capacity, acquiring a fibroblast phenotype. The transition of epithelium to fibroblastic phenotype is said to be driven by TGFβ1 (160). Therefore, the immunostaining of pSmad2/3 as mediators can reveal the TGFβ pathway possibly active. However, the results did not show significant difference for pSmad2/3 immunostaining for Rbm cells in current-smokers with COPD from non-smokers, but COPD ex-smokers did. This may indicate that even after quitting smoking, the pathogenesis of TGFβ pathway may work as a post-smoking effect. It may be also possible that the cells are initiating repairs and TGFβ can also function to induce this repair, as TGFβ is involved in normal physiological processes (132). Also, it would be worth looking at whether this repair process is occurring only in the Rbm and if it is, why only in this sub-epithelial layer and not in other areas. Cellularity is not the only change that is seen in the Rbm; changes in vascularity have also been noted in COPD patients (118, 137).

The current study showed that the current-smokers with COPD had a significant increase in pSmad2/3 immunostaining in the Rbm blood vessels from non-smokers, however, neither ex-smokers with COPD nor smokers with normal lung function were significantly different from non-smokers. Previous study has shown angiogenesis is hyperactive in the Rbm during airway remodelling in smokers with COPD, and TGFβ staining showed increased vessel-related upregulation in the blood vessels in the Rbm, supporting the active angiogenesis in the Rbm possibly through TGFβ pathway (65, 118). A number of studies have shown that TGFβ has angiogenic activities (161-163). An *in vivo* study showed that TGFβ can induce

angiogenesis (164). pSmad2/3 as a marker of the TGFβ pathway was increased in the blood vessels in this study, indicating the possibility of TGFβ acting through pSmad2/3 signaling in COPD current-smokers group. This pathological change may be reversible with smoking cessation, as the COPD ex-smokers group was not different from non-smokers group. Also, smoking alone may not cause pathogenesis, only when it is combined with the disease angiogenesis occurs.. Rbm is not the only sub-epithelial layer where vascular remodelling is seen in COPD patients; bronchial vascular remodelling is also seen in the lamina propria (LP) (61, 65, 137).

The current study found increased pSmad2/3 immunostaining in the blood vessels in LP in COPD groups compared to non-smokers. This complements previous work by Zanini et al who showed that TGFβ staining correlated significantly with vascular area. Calabrese *et al* reported more blood vessels in the LP of smokers and stated angiogenesis is a part of airway remodelling in smokers with COPD (165). This is contradicted by a study by Soltani *et al* which stated that the density of vessels in the LP was significantly lower than non-smokers (65). Zanini *et al* also showed larger vascular area in ex-smokers with moderate to severe COPD compared to control, but the number of vessels was not different between groups (137). These findings suggest that TGFβ is possibly acting through pSmad2/3 in the LP of COPD patients. Smoking cessation may cause reversible changes in angiogenesis in the Rbm, but not in LP. The increased activity of TGFβ pathway in the endothelial cells of the airways may be linked to increased Smad2/3 phosphorylation (60, 78, 166). The use of inhaled corticosteroids (ICS) is common in patients with COPD and therefore it is useful to evaluate whether the bronchial vascularity in patients with COPD is affected by the use of ICS.

ICS are widely used among a large proportion of COPD patients (167). The current study revealed that ICS did not change the pSmad2/3 immunostaining on blood vessels in COPD airways. Studies have shown effectiveness of ICS on airways remodelling in asthma, reducing thickness of Rbm and vessels in the mucosa in asthma (147, 148), but only a few studies have evaluated the role of ICS in COPD patients. Zanini *et al* showed that COPD patients treated with steroids had reduced vascular area and vessel size, but no effect on vessel numbers (137). Similarly, Soltani *et al* showed that ICS did not change the number of vessels in the airway mucosa (65). Zanini *et al* also showed TGFβ positive cells correlated significantly with vascular area and was less in people who were on ICS (137). However, the current study found no effect of ICS on Smad2/3 phosphorylation. It may be due to that inflammation is mostly treated with the anti-inflammatory effects of ICS; therefore it is more effective in asthma. Smoking, fibrosis and airway remodelling are major contributors to the aetiology of COPD in addition to inflammation. It has been suggested that COPD is 'resistant' to ICS (168). There are some studies that did not find any effects with ICS on clinical manifestations and airway inflammatory changes in COPD (167, 169). However, improvements in clinical symptoms, in quality of life, reduction of acute exacerbations, stabilisations of lung function have been reported in many studies (170-172). A potential limitation to this study that needs to be addressed is the small number of subjects in placebo groups. Therefore, further studies sampling more subjects are needed to clarify this further.

4.4 Future direction

TGFβ has been shown to mediate its effect by serine/threonine kinase activity (173), but it may also signal through other kinases. Study has shown integration of TGFβ and mitogen-activated protein kinase (MAPK) induces Smad phosphorylation (174). Also, it has been shown that TGFβ receptor activated extracellular signal regulated kinase (ERK) pathway, and resulted in increased Smad2 and Smad3 phosphorylation (175). TGFβ acts through multiple pathways, rather than one discrete pathway, and further studies of these pathways in COPD airways need to be conducted. Furthermore, future studies on pSmad2/3 immunostaining should measure total Smad2/3 proteins in order to analyse the ratio of pSmad2/3 to total Smad2/3 and the extent to which the proportion of pSmad2/3 immunostaining contributes to COPD airways. Additionally, some measures, such as measuring the Rbm thickness, total cellularity and vascularity in Rbm and LP may also indicate the proportion to which Smad2/3 are phosphorylated and their involvements. An interdisciplinary approach combining cellular, molecular and immunohistochemistry approaches is required to understand the precise role of phosphorylation of Smad2/3 in COPD airways and how it is possibly related to COPD pathogenesis.

4.5 Summary

In conclusion, my data suggest that TGFβ is possibly acting through pSmad2/3 signaling to induce changes in the epithelium, Rbm morphology, cellularity, and blood vessels in Rbm and LP in COPD airways, particularly in those who are smokers. In this regard, the epithelium and Rbm may be of particular pathological relevance in smokers and COPD, with the Rbm fragmentation, changes in vascularity, and migrating and transitioning epithelial cells through Rbm. TGFβ have been implicated in EMT in other situations, but there has been little specific work in the airways of smokers and COPD. Further studies are urgently required. Focusing on the profile of EMT-related transcription factors such as Smads will be a good way of distinguishing the likely active drivers such as TGFβ that act as intermediaries between the insult of cigarette smoke on the airway epithelium and downstream events which end with clinical phenotypes. Especially, the role of angiogenesis and possible EMT in smoking and/or COPD pathogenesis needs more research.

References:

1. Sohal SS, Ward C, Danial W, Wood-Baker R, Walters EH. Recent advances in understanding inflammation and remodeling in the airways in chronic obstructive pulmonary disease. Expert Rev Respir Med. 2013 Jun;7(3):275-88.
2. Laniado-Laborin R. Smoking and chronic obstructive pulmonary disease (COPD). Parallel epidemics of the 21 century. Int J Environ Res Public Health. 2009 Jan;6(1):209-24.
3. Toelle BG, Xuan W, Bird TE, Abramson MJ, Atkinson DN, Burton DL, et al. Respiratory symptoms and illness in older Australians: the Burden of Obstructive Lung Disease (BOLD) study. The Medical journal of Australia. 2013 Feb 18;198(3):144-8.
4. Lung Foundation Australia. COPD: The statistics 2012; Available from: http://www.lungfoundation.com.au/professional-resources/statistics/copd-the-statistics/.
5. COPD International. COPD Statistics 2002; Available from: http://www.copd-international.com/library/statistics.htm.
6. Deaths from chronic obstructive pulmonary disease--United States, 2000-2005. MMWR Morb Mortal Wkly Rep. 2008 Nov 14;57(45):1229-32.
7. Matheson MC, Raven J, Johns DP, Abramson MJ, Walters EH. Associations between reduced diffusing capacity and airflow obstruction in community-based subjects. Respir Med. 2007 Aug;101(8):1730-7.
8. National Heart, Lung, and Blood Institute. Global Initiative for Chronic Obstructive Lung Disease (GOLD). 2001
9. Walters EH, Walters J, Wills KE, Robinson A, Wood-Baker R. Clinical diaries in COPD: compliance and utility in predicting acute exacerbations. Int J Chron Obstruct Pulmon Dis. 2012;7:427-35.
10. Walters JA, Walters EH, Nelson M, Robinson A, Scott J, Turner P, et al. Factors associated with misdiagnosis of COPD in primary care. Prim Care Respir J. 2011 Dec;20(4):396-402.
11. Fletcher C, Peto R. The natural history of chronic airflow obstruction. Br Med J. 1977 Jun 25;1(6077):1645-8.
12. Yao H, Rahman I. Current concepts on oxidative/carbonyl stress, inflammation and epigenetics in pathogenesis of chronic obstructive pulmonary disease. Toxicol Appl Pharmacol. [Research Support, N.I.H., Extramural Review]. 2011 Jul 15;254(2):72-85.
13. Cosio MG, Saetta M, Agusti A. Immunologic aspects of chronic obstructive pulmonary disease. The New England journal of medicine. [Research Support, Non-U.S. Gov't Review]. 2009 Jun 4;360(23):2445-54.
14. Chung KF, Adcock IM. Multifaceted mechanisms in COPD: inflammation, immunity, and tissue repair and destruction. The European respiratory journal. [Review]. 2008 Jun;31(6):1334-56.
15. Perret JL, Dharmage SC, Matheson MC, Johns DP, Gurrin LC, Burgess JA, et al. The interplay between the effects of lifetime asthma, smoking, and atopy on fixed airflow obstruction in middle age. American journal of respiratory and critical care medicine. 2013 Jan 1;187(1):42-8.
16. Petty DT. The History of COPD. California, USA: Dr. Tom Petty 2005; Available from: http://www.perf2ndwind.org/html/news/2005/April-May/Page2.html.
17. Spriggs EA. John Hutchinson, the inventor of the spirometer--hisnorthcountrybackground, life in London, and scientific achievements. Med Hist. [Biography Historical Article]. 1977 Oct;21(4):357-64.
18. Reid L. Pathology of chronic bronchitis. Proc R Soc Med. 1956 Oct;49(10):771-3.
19. Reid L. Measurement of the bronchial mucous gland layer: a diagnostic yardstick in chronic bronchitis. Thorax. 1960 Jun;15:132-41.
20. O'Shaughnessy TC, Ansari TW, Barnes NC, Jeffery PK. Inflammation in bronchial biopsies of subjects with chronic bronchitis: inverse relationship of CD8+ T lymphocytes with FEV1. American journal of respiratory and critical care medicine. 1997 Mar;155(3):852-7.

21. Saetta M, Di Stefano A, Maestrelli P, Ferraresso A, Drigo R, Potena A, et al. Activated T-lymphocytes and macrophages in bronchial mucosa of subjects with chronic bronchitis. The American review of respiratory disease. 1993 Feb;147(2):301-6.
22. Norrby K. Mast cells and angiogenesis. APMIS. 2002 May;110(5):355-71.
23. Soltani A, Ewe YP, Lim ZS, Sohal SS, Reid D, Weston S, et al. Mast cells in COPD airways: relationship to bronchodilator responsiveness and angiogenesis. The European respiratory journal : official journal of the European Society for Clinical Respiratory Physiology. [Research Support, Non-U.S. Gov't]. 2012 Jun;39(6):1361-7.
24. Sohal SS, Reid D, Soltani A, Weston S, Muller HK, Wood-Baker R, et al. Changes in airway histone deacetylase2 in smokers and COPD with inhaled corticosteroids: a randomized controlled trial. PloS one. [Research Support, Non-U.S. Gov't]. 2013;8(5):e64833.
25. Sommerhoff CP, Nadel JA, Basbaum CB, Caughey GH. Neutrophil elastase and cathepsin G stimulate secretion from cultured bovine airway gland serous cells. The Journal of clinical investigation. [Research Support, Non-U.S. Gov't Research Support, U.S. Gov't, P.H.S.]. 1990 Mar;85(3):682-9.
26. SS Sohal, D Tan, HK Muller, DW Reid, EH Walters. Neutrophil numbers are decreased in bronchial biopsies from patients with COPD. Eur Respir J,. 2013; 42: Suppl. 57,: 104s.
27. Reid DW, Wen Y, Johns DP, Williams TJ, Ward C, Walters EH. Bronchodilator reversibility, airway eosinophilia and anti-inflammatory effects of inhaled fluticasone in COPD are not related. Respirology (Carlton, Vic). [Randomized Controlled Trial Research Support, Non-U.S. Gov't]. 2008 Nov;13(6):799-809.
28. McDonough JE, Yuan R, Suzuki M, Seyednejad N, Elliott WM, Sanchez PG, et al. Small-airway obstruction and emphysema in chronic obstructive pulmonary disease. The New England journal of medicine. 2011 Oct 27;365(17):1567-75.
29. Sohal SS, Reid D, Soltani A, Ward C, Weston S, Muller HK, et al. Reticular basement membrane fragmentation and potential epithelial mesenchymal transition is exaggerated in the airways of smokers with chronic obstructive pulmonary disease. Respirology. 2010 Aug;15(6):930-8.
30. Chen D, Gassenmaier M, Maruschke M, Riesenberg R, Pohla H, Stief CG, et al. Expression and prognostic significance of a comprehensive epithelial-mesenchymal transition gene set in renal cell carcinoma. J Urol. 2013 Sep 4.
31. Ding W, You H, Dang H, LeBlanc F, Galicia V, Lu SC, et al. Epithelial-to-mesenchymal transition of murine liver tumor cells promotes invasion. Hepatology. 2010 Sep;52(3):945-53.
32. Nakajima S, Doi R, Toyoda E, Tsuji S, Wada M, Koizumi M, et al. N-cadherin expression and epithelial-mesenchymal transition in pancreatic carcinoma. Clinical cancer research : an official journal of the American Association for Cancer Research. 2004 Jun 15;10(12 Pt 1):4125-33.
33. Zeng Q, Li W, Lu D, Wu Z, Duan H, Luo Y, et al. CD146, an epithelial-mesenchymal transition inducer, is associated with triple-negative breast cancer. Proceedings of the National Academy of Sciences of the United States of America. 2012 Jan 24;109(4):1127-32.
34. Thiery JP. Epithelial-mesenchymal transitions in tumour progression. Nat Rev Cancer. [Review]. 2002 Jun;2(6):442-54.
35. Young RP, Whittington CF, Hopkins RJ, Hay BA, Epton MJ, Black PN, et al. Chromosome 4q31 locus in COPD is also associated with lung cancer. The European respiratory journal : official journal of the European Society for Clinical Respiratory Physiology. 2010 Dec;36(6):1375-82.
36. Garcia Garcia Mdel C, Hernandez Borge J, Pires Goncalves P, Canon Barroso L, Molina Ortiz E, Castanar Jover A, et al. Cancer in Chronic Obstructive Pulmonary Disease (COPD) Patients. Chest. 2014 Mar 1;145(3 Suppl):422A.
37. De Craene B, Berx G. Regulatory networks defining EMT during cancer initiation and progression. Nat Rev Cancer. 2013 Feb;13(2):97-110.
38. Byers LA, Diao L, Wang J, Saintigny P, Girard L, Peyton M, et al. An epithelial-mesenchymal transition gene signature predicts resistance to EGFR and PI3K inhibitors and identifies Axl as a

therapeutic target for overcoming EGFR inhibitor resistance. Clinical cancer research : an official journal of the American Association for Cancer Research. 2013 Jan 1;19(1):279-90.
39. Hogg JC, Timens W. The pathology of chronic obstructive pulmonary disease. Annu Rev Pathol. [Research Support, N.I.H., Extramural Research Support, Non-U.S. Gov't Review]. 2009;4:435-59.
40. Southwell N. The aetiology, prevention and treatment of chronic bronchitis. Br J Ind Med. 1946 Apr;3:75-7.
41. Saetta M, Turato G, Baraldo S, Zanin A, Braccioni F, Mapp CE, et al. Goblet cell hyperplasia and epithelial inflammation in peripheral airways of smokers with both symptoms of chronic bronchitis and chronic airflow limitation. American journal of respiratory and critical care medicine. 2000 Mar;161(3 Pt 1):1016-21.
42. Vestbo J, Lange P. Can GOLD Stage 0 provide information of prognostic value in chronic obstructive pulmonary disease? American journal of respiratory and critical care medicine. 2002 Aug 1;166(3):329-32.
43. Hogg JC, Chu F, Utokaparch S, Woods R, Elliott WM, Buzatu L, et al. The nature of small-airway obstruction in chronic obstructive pulmonary disease. The New England journal of medicine. [Research Support, Non-U.S. Gov't Research Support, U.S. Gov't, Non-P.H.S. Research Support, U.S. Gov't, P.H.S.]. 2004 Jun 24;350(26):2645-53.
44. Macklem PT, Mead J. Resistance of central and peripheral airways measured by a retrograde catheter. Journal of applied physiology. 1967 Mar;22(3):395-401.
45. Wright JL, Lawson LM, Pare PD, Wiggs BJ, Kennedy S, Hogg JC. Morphology of peripheral airways in current smokers and ex-smokers. The American review of respiratory disease. [Comparative Study Research Support, Non-U.S. Gov't]. 1983 Apr;127(4):474-7.
46. Wright JL, Lawson LM, Pare PD, Kennedy S, Wiggs B, Hogg JC. The detection of small airways disease. The American review of respiratory disease. [Research Support, Non-U.S. Gov't]. 1984 Jun;129(6):989-94.
47. Hogg JC. Pathophysiology of airflow limitation in chronic obstructive pulmonary disease. Lancet. [Review]. 2004 Aug 21-27;364(9435):709-21.
48. Hogg JC, McDonough JE, Suzuki M. Small airway obstruction in COPD: new insights based on micro-CT imaging and MRI imaging. Chest. [Review]. 2013 May;143(5):1436-43.
49. Retamales I, Elliott WM, Meshi B, Coxson HO, Pare PD, Sciurba FC, et al. Amplification of inflammation in emphysema and its association with latent adenoviral infection. American journal of respiratory and critical care medicine. [Research Support, Non-U.S. Gov't Research Support, U.S. Gov't, P.H.S.]. 2001 Aug 1;164(3):469-73.
50. van den Berge M, ten Hacken NH, Cohen J, Douma WR, Postma DS. Small airway disease in asthma and COPD: clinical implications. Chest. 2011 Feb;139(2):412-23.
51. Vignola AM, Chanez P, Chiappara G, Merendino A, Pace E, Rizzo A, et al. Transforming growth factor-beta expression in mucosal biopsies in asthma and chronic bronchitis. American journal of respiratory and critical care medicine. 1997 Aug;156(2 Pt 1):591-9.
52. Dennler S, Goumans MJ, ten Dijke P. Transforming growth factor beta signal transduction. Journal of leukocyte biology. [Research Support, Non-U.S. Gov't Review]. 2002 May;71(5):731-40.
53. Sime PJ, O'Reilly KM. Fibrosis of the lung and other tissues: new concepts in pathogenesis and treatment. Clin Immunol. 2001 Jun;99(3):308-19.
54. Churg A, Tai H, Coulthard T, Wang R, Wright JL. Cigarette smoke drives small airway remodeling by induction of growth factors in the airway wall. American journal of respiratory and critical care medicine. 2006 Dec 15;174(12):1327-34.
55. Hogg JC, McDonough JE, Sanchez PG, Cooper JD, Coxson HO, Elliott WM, et al. Micro-computed tomography measurements of peripheral lung pathology in chronic obstructive pulmonary disease. Proceedings of the American Thoracic Society. 2009 Sep 15;6(6):546-9.
56. Sharafkhaneh A, Hanania NA, Kim V. Pathogenesis of emphysema: from the bench to the bedside. Proceedings of the American Thoracic Society. [Research Support, N.I.H., Extramural

Research Support, U.S. Gov't, Non-P.H.S. Research Support, U.S. Gov't, P.H.S. Review]. 2008 May 1;5(4):475-7.
57. MacNee W. Pathogenesis of chronic obstructive pulmonary disease. Proceedings of the American Thoracic Society. 2005;2(4):258-66; discussion 90-1.
58. Walters EH, Reid D, Soltani A, Ward C. Angiogenesis: a potentially critical part of remodelling in chronic airway diseases? Pharmacol Ther. 2008 Apr;118(1):128-37.
59. Sukhwinder S. Sohal, David Reid, Amir Soltani, Chris Ward, Steven Weston, H. Konrad Muller, et al. Reticular basement membrane fragmentation and potential epithelial-mesenchymal-transition is exaggerated in the airways of smokers with chronic obstructive pulmonary disease. . Respirology. 2010.
60. Raghu Kalluri, Robert A. Weinberg. The basics of epithelial-mesenchymal transition. The Journal of clinical investigation. 2009;119.
61. Soltani A, Muller HK, Sohal SS, Reid DW, Weston S, Wood-Baker R, et al. Distinctive characteristics of bronchial reticular basement membrane and vessel remodelling in chronic obstructive pulmonary disease (COPD) and in asthma: they are not the same disease. Histopathology. [Comparative Study]. 2012 May;60(6):964-70.
62. Sohal SS, Reid D, Soltani A, Ward C, Weston S, Muller HK, et al. Evaluation of epithelial mesenchymal transition in patients with chronic obstructive pulmonary disease. Respiratory research. [Comparative Study Evaluation Studies Research Support, Non-U.S. Gov't]. 2011;12:130.
63. Sohal SS, Walters EH. Role of epithelial mesenchymal transition (EMT) in chronic obstructive pulmonary disease (COPD). Respiratory research. 2013 Nov 6;14(1):120.
64. Sohal SS, Walters EH. Epithelial mesenchymal transition (EMT) in small airways of COPD patients. Thorax. 2013 Aug;68(8):783-4.
65. Soltani A, Reid DW, Sohal SS, Wood-Baker R, Weston S, Muller HK, et al. Basement membrane and vascular remodelling in smokers and chronic obstructive pulmonary disease: a cross-sectional study. Respiratory research. [Research Support, Non-U.S. Gov't]. 2010;11:105.
66. Wang Q, Wang Y, Zhang Y, Xiao W. The role of uPAR in epithelial-mesenchymal transition in small airway epithelium of patients with chronic obstructive pulmonary disease. Respiratory research. 2013;14:67.
67. Milara J, Peiro T, Serrano A, Cortijo J. Epithelial to mesenchymal transition is increased in patients with COPD and induced by cigarette smoke. Thorax. [Comparative Study Research Support, Non-U.S. Gov't]. 2013 May;68(5):410-20.
68. Camara J, Jarai G. Epithelial-mesenchymal transition in primary human bronchial epithelial cells is Smad-dependent and enhanced by fibronectin and TNF-alpha. Fibrogenesis Tissue Repair. 2010;3(1):2.
69. Kawashima K, Fujii T. Basic and clinical aspects of non-neuronal acetylcholine: overview of non-neuronal cholinergic systems and their biological significance. J Pharmacol Sci. 2008 Feb;106(2):167-73.
70. Undem BJ, Kollarik M. The role of vagal afferent nerves in chronic obstructive pulmonary disease. Proceedings of the American Thoracic Society. 2005;2(4):355-60; discussion 71-2.
71. Gosens R, Zaagsma J, Meurs H, Halayko AJ. Muscarinic receptor signaling in the pathophysiology of asthma and COPD. Respiratory research. 2006;7:73.
72. Gosens R, Zaagsma J, Grootte Bromhaar M, Nelemans A, Meurs H. Acetylcholine: a novel regulator of airway smooth muscle remodelling? Eur J Pharmacol. 2004 Oct 1;500(1-3):193-201.
73. Milara J, Serrano A, Peiro T, Gavalda A, Miralpeix M, Morcillo EJ, et al. Aclidinium inhibits human lung fibroblast to myofibroblast transition. Thorax. 2012 Mar;67(3):229-37.
74. Milara J, Serrano A, Peiro T, Artigues E, Gavalda A, Miralpeix M, et al. Aclidinium inhibits cigarette smoke-induced lung fibroblast-to-myofibroblast transition. The European respiratory journal : official journal of the European Society for Clinical Respiratory Physiology. 2013 Jun;41(6):1264-74.

75. Asano K, Shikama Y, Shoji N, Hirano K, Suzaki H, Nakajima H. Tiotropium bromide inhibits TGF-beta-induced MMP production from lung fibroblasts by interfering with Smad and MAPK pathways in vitro. Int J Chron Obstruct Pulmon Dis. 2010;5:277-86.
76. Yang K, Song Y, Tang YB, Xu ZP, Zhou W, Hou LN, et al. mAChRs activation induces epithelial-mesenchymal transition on lung epithelial cells. BMC Pulm Med. 2014;14:53.
77. Hay ED. An overview of epithelio-mesenchymal transformation. Acta anatomica. [Research Support, U.S. Gov't, P.H.S. Review]. 1995;154(1):8-20.
78. Kalluri R, Neilson EG. Epithelial-mesenchymal transition and its implications for fibrosis. The Journal of clinical investigation. [Research Support, Non-U.S. Gov't Research Support, U.S. Gov't, P.H.S. Review]. 2003 Dec;112(12):1776-84.
79. Thiery JP, Acloque H, Huang RY, Nieto MA. Epithelial-mesenchymal transitions in development and disease. Cell. 2009 Nov 25;139(5):871-90.
80. Iwano M, Plieth D, Danoff TM, Xue C, Okada H, Neilson EG. Evidence that fibroblasts derive from epithelium during tissue fibrosis. The Journal of clinical investigation. [Research Support, U.S. Gov't, P.H.S.]. 2002 Aug;110(3):341-50.
81. Willis BC, Borok Z. TGF-beta-induced EMT: mechanisms and implications for fibrotic lung disease. American journal of physiology Lung cellular and molecular physiology. 2007 Sep;293(3):L525-34.
82. Xu J, Lamouille S, Derynck R. TGF-beta-induced epithelial to mesenchymal transition. Cell Res. 2009 Feb;19(2):156-72.
83. Kim MK, Maeng YI, Sung WJ, Oh HK, Park JB, Yoon GS, et al. The differential expression of TGF-beta1, ILK and wnt signaling inducing epithelial to mesenchymal transition in human renal fibrogenesis: an immunohistochemical study. Int J Clin Exp Pathol. [Research Support, Non-U.S. Gov't]. 2013;6(9):1747-58.
84. Takizawa H, Tanaka M, Takami K, Ohtoshi T, Ito K, Satoh M, et al. Increased expression of transforming growth factor-beta1 in small airway epithelium from tobacco smokers and patients with chronic obstructive pulmonary disease (COPD). American journal of respiratory and critical care medicine. 2001 May;163(6):1476-83.
85. Zhang M, Zhang Z, Pan HY, Wang DX, Deng ZT, Ye XL. TGF-beta1 induces human bronchial epithelial cell-to-mesenchymal transition in vitro. Lung. 2009 May-Jun;187(3):187-94.
86. Fan JM, Ng YY, Hill PA, Nikolic-Paterson DJ, Mu W, Atkins RC, et al. Transforming growth factor-beta regulates tubular epithelial-myofibroblast transdifferentiation in vitro. Kidney Int. [In Vitro Research Support, Non-U.S. Gov't]. 1999 Oct;56(4):1455-67.
87. Kasai H, Allen JT, Mason RM, Kamimura T, Zhang Z. TGF-beta1 induces human alveolar epithelial to mesenchymal cell transition (EMT). Respiratory research. [Research Support, Non-U.S. Gov't]. 2005;6:56.
88. Kim KK, Kugler MC, Wolters PJ, Robillard L, Galvez MG, Brumwell AN, et al. Alveolar epithelial cell mesenchymal transition develops in vivo during pulmonary fibrosis and is regulated by the extracellular matrix. Proceedings of the National Academy of Sciences of the United States of America. [Research Support, N.I.H., Extramural]. 2006 Aug 29;103(35):13180-5.
89. Flanders KC. Smad3 as a mediator of the fibrotic response. Int J Exp Pathol. [Review]. 2004 Apr;85(2):47-64.
90. Miyazawa K, Shinozaki M, Hara T, Furuya T, Miyazono K. Two major Smad pathways in TGF-beta superfamily signalling. Genes Cells. [Research Support, Non-U.S. Gov't Review]. 2002 Dec;7(12):1191-204.
91. Ju W, Ogawa A, Heyer J, Nierhof D, Yu L, Kucherlapati R, et al. Deletion of Smad2 in mouse liver reveals novel functions in hepatocyte growth and differentiation. Mol Cell Biol. [Research Support, N.I.H., Extramural Research Support, Non-U.S. Gov't]. 2006 Jan;26(2):654-67.
92. Zavadil J, Bottinger EP. TGF-beta and epithelial-to-mesenchymal transitions. Oncogene. [Research Support, N.I.H., Extramural Research Support, U.S. Gov't, P.H.S. Review]. 2005 Aug 29;24(37):5764-74.

93. Tian F, DaCosta Byfield S, Parks WT, Yoo S, Felici A, Tang B, et al. Reduction in Smad2/3 signaling enhances tumorigenesis but suppresses metastasis of breast cancer cell lines. Cancer research. 2003 Dec 1;63(23):8284-92.
94. Bakin AV, Tomlinson AK, Bhowmick NA, Moses HL, Arteaga CL. Phosphatidylinositol 3-kinase function is required for transforming growth factor beta-mediated epithelial to mesenchymal transition and cell migration. The Journal of biological chemistry. 2000 Nov 24;275(47):36803-10.
95. Lien SC, Usami S, Chien S, Chiu JJ. Phosphatidylinositol 3-kinase/Akt pathway is involved in transforming growth factor-beta1-induced phenotypic modulation of 10T1/2 cells to smooth muscle cells. Cell Signal. 2006 Aug;18(8):1270-8.
96. Kattla JJ, Carew RM, Heljic M, Godson C, Brazil DP. Protein kinase B/Akt activity is involved in renal TGF-beta1-driven epithelial-mesenchymal transition in vitro and in vivo. Am J Physiol Renal Physiol. 2008 Jul;295(1):F215-25.
97. Zavadil J, Bitzer M, Liang D, Yang YC, Massimi A, Kneitz S, et al. Genetic programs of epithelial cell plasticity directed by transforming growth factor-beta. Proceedings of the National Academy of Sciences of the United States of America. 2001 Jun 5;98(12):6686-91.
98. Rao VN, Reddy ES. elk-1 proteins interact with MAP kinases. Oncogene. 1994 Jul;9(7):1855-60.
99. Boutet A, De Frutos CA, Maxwell PH, Mayol MJ, Romero J, Nieto MA. Snail activation disrupts tissue homeostasis and induces fibrosis in the adult kidney. The EMBO journal. [Research Support, Non-U.S. Gov't]. 2006 Nov 29;25(23):5603-13.
100. Dhasarathy A, Phadke D, Mav D, Shah RR, Wade PA. The transcription factors Snail and Slug activate the transforming growth factor-beta signaling pathway in breast cancer. PloS one. [Research Support, N.I.H., Extramural Research Support, N.I.H., Intramural]. 2011;6(10):e26514.
101. Kang H, Lee M, Jang SW. Celastrol inhibits TGF-beta1-induced epithelial-mesenchymal transition by inhibiting Snail and regulating E-cadherin expression. Biochemical and biophysical research communications. 2013 Aug 9;437(4):550-6.
102. Medici D, Hay ED, Olsen BR. Snail and Slug promote epithelial-mesenchymal transition through beta-catenin-T-cell factor-4-dependent expression of transforming growth factor-beta3. Molecular biology of the cell. [Research Support, N.I.H., Extramural]. 2008 Nov;19(11):4875-87.
103. Yang J, Mani SA, Donaher JL, Ramaswamy S, Itzykson RA, Come C, et al. Twist, a master regulator of morphogenesis, plays an essential role in tumor metastasis. Cell. [Research Support, Non-U.S. Gov't Research Support, U.S. Gov't, Non-P.H.S. Research Support, U.S. Gov't, P.H.S.]. 2004 Jun 25;117(7):927-39.
104. Nusse R, Varmus H. Three decades of Wnts: a personal perspective on how a scientific field developed. The EMBO journal. 2012 Jun 13;31(12):2670-84.
105. Woll PS, Morris JK, Painschab MS, Marcus RK, Kohn AD, Biechele TL, et al. Wnt signaling promotes hematoendothelial cell development from human embryonic stem cells. Blood. 2008 Jan 1;111(1):122-31.
106. Angers S, Moon RT. Proximal events in Wnt signal transduction. Nat Rev Mol Cell Biol. 2009 Jul;10(7):468-77.
107. Sarkar FH, Li Y, Wang Z, Kong D. The role of nutraceuticals in the regulation of Wnt and Hedgehog signaling in cancer. Cancer Metastasis Rev. 2010 Sep;29(3):383-94.
108. Kim K, Lu Z, Hay ED. Direct evidence for a role of beta-catenin/LEF-1 signaling pathway in induction of EMT. Cell Biol Int. 2002;26(5):463-76.
109. Fuxe J, Karlsson MC. TGF-beta-induced epithelial-mesenchymal transition: a link between cancer and inflammation. Semin Cancer Biol. 2012 Oct;22(5-6):455-61.
110. Yang L, Xie G, Fan Q, Xie J. Activation of the hedgehog-signaling pathway in human cancer and the clinical implications. Oncogene. 2010 Jan 28;29(4):469-81.
111. Hannigan G, Troussard AA, Dedhar S. Integrin-linked kinase: a cancer therapeutic target unique among its ILK. Nat Rev Cancer. 2005 Jan;5(1):51-63.

112. Chen D, Zhang Y, Zhang X, Li J, Han B, Liu S, et al. Overexpression of integrin-linked kinase correlates with malignant phenotype in non-small cell lung cancer and promotes lung cancer cell invasion and migration via regulating epithelial-mesenchymal transition (EMT)-related genes. Acta Histochem. 2013 Mar;115(2):128-36.
113. Margadant C, Sonnenberg A. Integrin-TGF-beta crosstalk in fibrosis, cancer and wound healing. EMBO Rep. 2010 Feb;11(2):97-105.
114. Chandrasekar N, Mohanam S, Gujrati M, Olivero WC, Dinh DH, Rao JS. Downregulation of uPA inhibits migration and PI3k/Akt signaling in glioblastoma cells. Oncogene. 2003 Jan 23;22(3):392-400.
115. Jo M, Lester RD, Montel V, Eastman B, Takimoto S, Gonias SL. Reversibility of epithelial-mesenchymal transition (EMT) induced in breast cancer cells by activation of urokinase receptor-dependent cell signaling. The Journal of biological chemistry. 2009 Aug 21;284(34):22825-33.
116. Lester RD, Jo M, Montel V, Takimoto S, Gonias SL. uPAR induces epithelial-mesenchymal transition in hypoxic breast cancer cells. The Journal of cell biology. 2007 Jul 30;178(3):425-36.
117. Larue L, Bellacosa A. Epithelial-mesenchymal transition in development and cancer: role of phosphatidylinositol 3' kinase/AKT pathways. Oncogene. 2005 Nov 14;24(50):7443-54.
118. Soltani A, Sohal SS, Reid D, Weston S, Wood-Baker R, Walters EH. Vessel-associated transforming growth factor-beta1 (TGF-beta1) is increased in the bronchial reticular basement membrane in COPD and normal smokers. PloS one. [Research Support, Non-U.S. Gov't]. 2012;7(6):e39736.
119. Ponce CC, de Lourdes Lopes Ferrari Chauffaille M, Ihara SS, Silva MR. Increased angiogenesis in primary myelofibrosis: latent transforming growth factor-beta as a possible angiogenic factor. Rev Bras Hematol Hemoter. 2014 Sep-Oct;36(5):322-8.
120. Kranenburg AR, de Boer WI, Alagappan VK, Sterk PJ, Sharma HS. Enhanced bronchial expression of vascular endothelial growth factor and receptors (Flk-1 and Flt-1) in patients with chronic obstructive pulmonary disease. Thorax. 2005 Feb;60(2):106-13.
121. Wright JL, Tai H, Churg A. Cigarette smoke induces persisting increases of vasoactive mediators in pulmonary arteries. Am J Respir Cell Mol Biol. 2004 Nov;31(5):501-9.
122. Wen FQ, Liu X, Manda W, Terasaki Y, Kobayashi T, Abe S, et al. TH2 Cytokine-enhanced and TGF-beta-enhanced vascular endothelial growth factor production by cultured human airway smooth muscle cells is attenuated by IFN-gamma and corticosteroids. The Journal of allergy and clinical immunology. 2003 Jun;111(6):1307-18.
123. Heldin CH, Miyazono K, ten Dijke P. TGF-beta signalling from cell membrane to nucleus through SMAD proteins. Nature. 1997 Dec 4;390(6659):465-71.
124. Savage C, Das P, Finelli AL, Townsend SR, Sun CY, Baird SE, et al. Caenorhabditis elegans genes sma-2, sma-3, and sma-4 define a conserved family of transforming growth factor beta pathway components. Proceedings of the National Academy of Sciences of the United States of America. 1996 Jan 23;93(2):790-4.
125. Gong Y, Guo Y, Hai Y, Yang H, Liu Y, Yang S, et al. Nodal promotes the self-renewal of human colon cancer stem cells via an autocrine manner through Smad2/3 signaling pathway. Biomed Res Int. 2014;2014:364134.
126. Arteaga CL, Coffey RJ, Jr., Dugger TC, McCutchen CM, Moses HL, Lyons RM. Growth stimulation of human breast cancer cells with anti-transforming growth factor beta antibodies: evidence for negative autocrine regulation by transforming growth factor beta. Cell Growth Differ. 1990 Aug;1(8):367-74.
127. Jakowlew SB. Transforming growth factor-beta in cancer and metastasis. Cancer Metastasis Rev. 2006 Sep;25(3):435-57.
128. Bretland AJ, Reid SV, Chapple CR, Eaton CL. Role of endogenous transforming growth factor beta (TGFbeta)1 in prostatic stromal cells. Prostate. 2001 Sep 15;48(4):297-304.

129. Story MT, Hopp KA, Meier DA. Regulation of basic fibroblast growth factor expression by transforming growth factor beta in cultured human prostate stromal cells. Prostate. 1996 Apr;28(4):219-26.
130. Zhang YE. Non-Smad pathways in TGF-beta signaling. Cell Res. [Research Support, N.I.H., Intramural Review]. 2009 Jan;19(1):128-39.
131. Yeh YY, Chiao CC, Kuo WY, Hsiao YC, Chen YJ, Wei YY, et al. TGF-beta1 increases motility and alphavbeta3 integrin up-regulation via PI3K, Akt and NF-kappaB-dependent pathway in human chondrosarcoma cells. Biochemical pharmacology. 2008 Mar 15;75(6):1292-301.
132. Massague J. TGF-beta signal transduction. Annu Rev Biochem. 1998;67:753-91.
133. Massague J, Seoane J, Wotton D. Smad transcription factors. Genes Dev. 2005 Dec 1;19(23):2783-810.
134. N Danial. Epithelial mesenchymal transition in the small and large airways of patients with lung cancer. [Honours Thesis]. Hobart: School of Medicine, University of Tasmania 2012.
135. Beghe B, Bazzan E, Baraldo S, Calabrese F, Rea F, Loy M, et al. Transforming growth factor-beta type II receptor in pulmonary arteries of patients with very severe COPD. The European respiratory journal : official journal of the European Society for Clinical Respiratory Physiology. 2006 Sep;28(3):556-62.
136. Suissa S, Barnes PJ. Inhaled corticosteroids in COPD: the case against. The European respiratory journal : official journal of the European Society for Clinical Respiratory Physiology. 2009 Jul;34(1):13-6.
137. Zanini A, Chetta A, Saetta M, Baraldo S, Castagnetti C, Nicolini G, et al. Bronchial vascular remodelling in patients with COPD and its relationship with inhaled steroid treatment. Thorax. 2009 Dec;64(12):1019-24.
138. Kirkham S, Kolsum U, Rousseau K, Singh D, Vestbo J, Thornton DJ. MUC5B is the major mucin in the gel phase of sputum in chronic obstructive pulmonary disease. American journal of respiratory and critical care medicine. 2008 Nov 15;178(10):1033-9.
139. Baraldo S, Turato G, Saetta M. Pathophysiology of the small airways in chronic obstructive pulmonary disease. Respiration; international review of thoracic diseases. [Review]. 2012;84(2):89-97.
140. Cosio Piqueras MG, Cosio MG. Disease of the airways in chronic obstructive pulmonary disease. Eur Respir J Suppl. 2001 Dec;34:41s-9s.
141. Shi Y, Massague J. Mechanisms of TGF-beta signaling from cell membrane to the nucleus. Cell. 2003 Jun 13;113(6):685-700.
142. Kolosova I, Nethery D, Kern JA. Role of Smad2/3 and p38 MAP kinase in TGF-beta1-induced epithelial-mesenchymal transition of pulmonary epithelial cells. J Cell Physiol. 2011 May;226(5):1248-54.
143. Crystal RG. Airway basal cells. The "smoking gun" of chronic obstructive pulmonary disease. American journal of respiratory and critical care medicine. 2014 Dec 15;190(12):1355-62.
144. Satelli A, Li S. Vimentin in cancer and its potential as a molecular target for cancer therapy. Cell Mol Life Sci. 2011 Sep;68(18):3033-46.
145. Yang IA, Clarke MS, Sim EH, Fong KM. Inhaled corticosteroids for stable chronic obstructive pulmonary disease. Cochrane Database Syst Rev. 2012;7:CD002991.
146. Falk JA, Minai OA, Mosenifar Z. Inhaled and systemic corticosteroids in chronic obstructive pulmonary disease. Proceedings of the American Thoracic Society. 2008 May 1;5(4):506-12.
147. Olivieri D, Chetta A, Del Donno M, Bertorelli G, Casalini A, Pesci A, et al. Effect of short-term treatment with low-dose inhaled fluticasone propionate on airway inflammation and remodeling in mild asthma: a placebo-controlled study. American journal of respiratory and critical care medicine. 1997 Jun;155(6):1864-71.
148. Ward C, Pais M, Bish R, Reid D, Feltis B, Johns D, et al. Airway inflammation, basement membrane thickening and bronchial hyperresponsiveness in asthma. Thorax. 2002 Apr;57(4):309-16.

149. Hogan BL, Barkauskas CE, Chapman HA, Epstein JA, Jain R, Hsia CC, et al. Repair and regeneration of the respiratory system: complexity, plasticity, and mechanisms of lung stem cell function. Cell Stem Cell. 2014 Aug 7;15(2):123-38.
150. Barkauskas CE, Cronce MJ, Rackley CR, Bowie EJ, Keene DR, Stripp BR, et al. Type 2 alveolar cells are stem cells in adult lung. The Journal of clinical investigation. 2013 Jul;123(7):3025-36.
151. Araya J, Cambier S, Markovics JA, Wolters P, Jablons D, Hill A, et al. Squamous metaplasia amplifies pathologic epithelial-mesenchymal interactions in COPD patients. The Journal of clinical investigation. 2007 Nov;117(11):3551-62.
152. Kim V, Rogers TJ, Criner GJ. New concepts in the pathobiology of chronic obstructive pulmonary disease. Proceedings of the American Thoracic Society. 2008 May 1;5(4):478-85.
153. Thorley AJ, Tetley TD. Pulmonary epithelium, cigarette smoke, and chronic obstructive pulmonary disease. Int J Chron Obstruct Pulmon Dis. 2007;2(4):409-28.
154. Ghosh AK. Factors involved in the regulation of type I collagen gene expression: implication in fibrosis. Exp Biol Med (Maywood). 2002 May;227(5):301-14.
155. Saika S, Kono-Saika S, Tanaka T, Yamanaka O, Ohnishi Y, Sato M, et al. Smad3 is required for dedifferentiation of retinal pigment epithelium following retinal detachment in mice. Lab Invest. 2004 Oct;84(10):1245-58.
156. Sato M, Muragaki Y, Saika S, Roberts AB, Ooshima A. Targeted disruption of TGF-beta1/Smad3 signaling protects against renal tubulointerstitial fibrosis induced by unilateral ureteral obstruction. The Journal of clinical investigation. 2003 Nov;112(10):1486-94.
157. Liesker JJ, Ten Hacken NH, Zeinstra-Smith M, Rutgers SR, Postma DS, Timens W. Reticular basement membrane in asthma and COPD: similar thickness, yet different composition. Int J Chron Obstruct Pulmon Dis. 2009;4:127-35.
158. Jeffery PK. Remodeling and inflammation of bronchi in asthma and chronic obstructive pulmonary disease. Proceedings of the American Thoracic Society. 2004;1(3):176-83.
159. Chanez P, Vignola AM, O'Shaugnessy T, Enander I, Li D, Jeffery PK, et al. Corticosteroid reversibility in COPD is related to features of asthma. American journal of respiratory and critical care medicine. 1997 May;155(5):1529-34.
160. Cheng S, Lovett DH. Gelatinase A (MMP-2) is necessary and sufficient for renal tubular cell epithelial-mesenchymal transformation. The American journal of pathology. [Research Support, Non-U.S. Gov't]. 2003 Jun;162(6):1937-49.
161. Jackson JR, Seed MP, Kircher CH, Willoughby DA, Winkler JD. The codependence of angiogenesis and chronic inflammation. FASEB J. 1997 May;11(6):457-65.
162. Klagsbrun M, D'Amore PA. Regulators of angiogenesis. Annu Rev Physiol. 1991;53:217-39.
163. Puxeddu I, Ribatti D, Crivellato E, Levi-Schaffer F. Mast cells and eosinophils: a novel link between inflammation and angiogenesis in allergic diseases. The Journal of allergy and clinical immunology. 2005 Sep;116(3):531-6.
164. Roberts AB, Sporn MB, Assoian RK, Smith JM, Roche NS, Wakefield LM, et al. Transforming growth factor type beta: rapid induction of fibrosis and angiogenesis in vivo and stimulation of collagen formation in vitro. Proceedings of the National Academy of Sciences of the United States of America. 1986 Jun;83(12):4167-71.
165. Calabrese C, Bocchino V, Vatrella A, Marzo C, Guarino C, Mascitti S, et al. Evidence of angiogenesis in bronchial biopsies of smokers with and without airway obstruction. Respir Med. 2006 Aug;100(8):1415-22.
166. Lee JM, Dedhar S, Kalluri R, Thompson EW. The epithelial-mesenchymal transition: new insights in signaling, development, and disease. The Journal of cell biology. [Research Support, N.I.H., Extramural Research Support, Non-U.S. Gov't Research Support, U.S. Gov't, Non-P.H.S. Review]. 2006 Mar 27;172(7):973-81.
167. Rodrigo GJ, Castro-Rodriguez JA, Plaza V. Safety and efficacy of combined long-acting beta-agonists and inhaled corticosteroids vs long-acting beta-agonists monotherapy for stable COPD: a systematic review. Chest. 2009 Oct;136(4):1029-38.

168. To Y, Ito K, Kizawa Y, Failla M, Ito M, Kusama T, et al. Targeting phosphoinositide-3-kinase-delta with theophylline reverses corticosteroid insensitivity in chronic obstructive pulmonary disease. American journal of respiratory and critical care medicine. 2010 Oct 1;182(7):897-904.
169. Vestbo J, Sorensen T, Lange P, Brix A, Torre P, Viskum K. Long-term effect of inhaled budesonide in mild and moderate chronic obstructive pulmonary disease: a randomised controlled trial. Lancet. 1999 May 29;353(9167):1819-23.
170. Aaron SD, Vandemheen KL, Fergusson D, Maltais F, Bourbeau J, Goldstein R, et al. Tiotropium in combination with placebo, salmeterol, or fluticasone-salmeterol for treatment of chronic obstructive pulmonary disease: a randomized trial. Annals of internal medicine. 2007 Apr 17;146(8):545-55.
171. Calverley PM, Anderson JA, Celli B, Ferguson GT, Jenkins C, Jones PW, et al. Salmeterol and fluticasone propionate and survival in chronic obstructive pulmonary disease. The New England journal of medicine. 2007 Feb 22;356(8):775-89.
172. Wedzicha JA, Calverley PM, Seemungal TA, Hagan G, Ansari Z, Stockley RA. The prevention of chronic obstructive pulmonary disease exacerbations by salmeterol/fluticasone propionate or tiotropium bromide. American journal of respiratory and critical care medicine. 2008 Jan 1;177(1):19-26.
173. Atfi A, Lepage K, Allard P, Chapdelaine A, Chevalier S. Activation of a serine/threonine kinase signaling pathway by transforming growth factor type beta. Proceedings of the National Academy of Sciences of the United States of America. 1995 Dec 19;92(26):12110-4.
174. Cordenonsi M, Montagner M, Adorno M, Zacchigna L, Martello G, Mamidi A, et al. Integration of TGF-beta and Ras/MAPK signaling through p53 phosphorylation. Science. 2007 Feb 9;315(5813):840-3.
175. Hough C, Radu M, Dore JJ. Tgf-beta induced Erk phosphorylation of smad linker region regulates smad signaling. PloS one. 2012;7(8):e42513.

Appendix 1: The epithelial cells raw data.

NC	Number of Smad cells	Std	Total number of cells	Std	Rbm length (μm)	Std
1	48.2	10.35	52.8	11.08	588.95	80.91
2	167	83.12	185	90.35	652.53	207.02
3	92.4	55.21	97.8	56.53	503.97	264.35
4	183.4	90.28	204.4	87.28	502.11	166.88
5	32	9.59	61.6	25.38	528.05	101.39
6	103.6	33.71	141.6	54.61	556.91	102.99
7	81.6	33.58	94	37.21	485.80	121.04
8	120.4	42.44	126.2	44.01	470.37	77.09
9	99	15.60	119.4	18.20	616.81	201.27
10	57.2	11.97	62.6	14.24	467.75	132.19
11	105.4	43.46	116.2	54.13	479.24	150.51
12	107.2	58.17	115.8	58.60	604.62	249.98
Mean	99.78 (32-183)	40.62	114.78 (53-204)	45.97	538.09 (468-653)	154.63
NLFS	Number of Smad cells	Std	Total number of cells	Std	Rbm length (μm)	Std
1	62.2	27.23	63.2	27.82	325.56	31.96
2	63.2	14.92	66	15.25	376.54	64.54
3	26	19.20	29.2	20.13	319.39	167.18
4	30.8	10.92	34.2	11.56	458.82	125.28
5	74.6	39.88	85.2	46.53	387.01	45.57
6	87.6	18.26	91.8	16.90	415.04	132.98
7	48.4	39.64	70.6	40.06	414.60	156.27
8	99.6	33.05	103.2	36.62	397.59	55.39
9	86.6	44.67	91.4	46.57	394.38	94.37
10	24.8	12.56	25.2	12.28	415.17	64.56
11	185.2	64.05	195	63.05	438.34	67.99
12	103.6	23.14	106.4	24.57	342.31	85.34
13	155.8	30.27	162.6	37.20	444.45	92.90
Mean	80.65 (25-185)	29.06	86.46 (25-195)	30.66	394.55 (319-459)	91.10
COPD CS	Number of Smad cells	Std	Total number of cells	Std	Rbm length (μm)	Std
1	233.2	79.42	235.2	80.24	582.25	130.05
2	106.8	53.43	108	53.76	346.48	53.75
3	32	14.95	34.2	15.69	366.47	131.49
4	150.4	69.42	154	70.20	592.49	200.08
5	30.6	8.32	46	19.77	446.54	134.27
6	133.4	42.78	143	50.26	554.68	81.90
7	116.4	39.37	117	39.04	453.53	104.89
8	42.6	7.33	45.4	8.02	372.15	39.13
9	98.4	61.74	99.6	61.44	405.50	98.45

10	97.8	46.85	98.4	46.92	675.43	197.89
11	71.8	19.54	79	16.78	626.96	116.04
12	115.4	67.76	116.4	67.15	432.76	78.90
13	45.2	25.47	46.4	25.91	355.70	63.31
14	38	12.51	38	12.51	398.55	119.73
15	18.4	6.91	19.2	6.94	327.99	113.49
Mean	88.69 (18-233)	37.05	91.99 (19-235)	38.31	462.50 (328-675)	110.89
COPDES	Number of Smad cells	Std	Total number of cells	Std	Rbm length (μm)	Std
1	131.4	25.43	137	31.18	441.91	139.45
2	72.6	15.37	74.4	14.60	465.83	78.79
3	41.8	16.44	42.2	16.24	388.75	100.46
4	140.4	25.09	141.6	25.04	500.17	159.26
5	81.8	48.44	83.6	50.47	425.76	140.67
6	70.6	18.76	71.4	18.32	377.95	89.52
7	69.4	19.03	70	19.66	423.14	72.87
8	175	27.82	198	33.40	500.71	133.06
9	72.8	14.04	73.4	14.12	430.80	65.57
10	88.4	15.73	90	15.22	557.95	164.65
11	106.4	92.65	110.8	95.01	419.73	142.36
12	82.6	31.51	83.2	31.22	416.08	66.55
Mean	94.43 (42-175)	29.19	97.97 (42-198)	30.37	445.73 (378-558)	112.77